A&A 548, A102 (2012)
DOI: 10.1051/0004-6361/201218993

Astronomy & Astrophysics

Towards an understanding of third-order galaxy-galaxy lensing

P. Simon, P. Schneider, and D. Kübler

Argelander-Institut für Astronomie, Universität Bonn, Auf dem Hügel 71, 53121 Bonn, Germany
e-mail: psimon@astro.uni-bonn.de

Received 8 February 2012 / Accepted 17 October 2012

ABSTRACT

Context. Third-order galaxy-galaxy lensing (G3L) is a next generation galaxy-galaxy lensing (GGL) technique that either measures the excess shear about lens pairs or the excess shear-shear correlations about lenses. From their definition it is clear that these statistics assess the three-point correlations between galaxy positions and projected matter density.
Aims. For future applications of these novel statistics, we aim at a more intuitive understanding of G3L to isolate the main features that possibly can be measured.
Methods. We construct a toy model ("isolated lens model"; ILM) for the distribution of galaxies and associated matter to determine the measured quantities of the two G3L correlation functions and traditional GGL in a simplified context. The ILM presumes single lens galaxies to be embedded inside arbitrary matter haloes that, however, are statistically independent ("isolated") from any other halo or lens position. Clusters of galaxies and their common cluster matter haloes are a consequence of clustering smaller haloes. In particular, the average mass-to-galaxy number ratio of clusters of any size cannot change in the ILM.
Results. GGL and galaxy clustering alone cannot distinguish an ILM from any more complex scenario. The lens-lens-shear correlator in combination with second-order statistics enables us to detect deviations from a ILM, though. This can be quantified by a difference signal defined in the paper. We demonstrate with the ILM that this correlator picks up the excess matter distribution about galaxy pairs inside clusters, whereas pairs with lenses well separated in redshift only suppress the overall amplitude of the correlator. The amplitude suppression can be normalised. The lens-lens-shear correlator is sensitive to variations among matter haloes. In principle, it could be devised to constrain the ellipticities of haloes, without the need for luminous tracers, or maybe even random halo substructure.

Key words. gravitational lensing: weak – galaxies: halos – large-scale structure of Universe

1. Introduction

Gravitational lensing (Schneider 2006, for a recent review) has established itself as valuable tool for cosmology to investigate the large-scale distribution of matter and its relation to visible tracers such as galaxies. In the currently favoured standard model of cosmology (e.g., Peebles 1993; Dodelson 2003), the major fraction of matter is a non-baryonic cold dark matter component, i.e., matter with non-relativistic velocities during the epoch of cosmic structure formation. In this situation, gravitational lensing is an excellent probe as it is sensitive to all matter as long as it interacts gravitationally.

The main observable in lensing is the distortion of shapes of galaxy images, in the weak lensing regime mainly "shear", by the intervening inhomogeneous gravitational potential that is traversed by light bundles from the galaxy. Over the course of the past decade, applications of the gravitational lensing effect have come of age. To name a few results (Bartelmann 2010, and references therein), it was used to map the dark matter distribution, to study the matter density profiles in galaxy clusters and to determine their masses, to measure the relation between the galaxy and dark matter distribution (the so-called galaxy bias), to constrain the total matter density of the Universe and its fluctuation power spectrum, and very recently to gather independent evidence for the overall accelerated expansion of the cosmos (Schrabback et al. 2010).

Of particular interest for this paper is the so-called galaxy-galaxy lensing (GGL) technique where positions of foreground galaxies ("lenses") are correlated with the (weak lensing) shear on background galaxy images ("sources"). Thereby, statistical information on the projected matter distribution around lens galaxies can be extracted. Since the first attempt by Tyson et al. (1984) and the first detection (Brainerd et al. 1996; Griffiths et al. 1996) of this effect, GGL nowadays is a widely applied robust method to study the galaxy-matter connection (Fischer et al. 2000; McKay et al. 2001; Guzik & Seljak 2002; Hoekstra et al. 2002, 2004; Pen et al. 2003; Seljak & Warren 2004; Sheldon et al. 2004; Mandelbaum et al. 2005; Kleinheinrich et al. 2005; Mandelbaum et al. 2006b,a; Simon et al. 2007; Parker et al. 2007; van Uitert et al. 2011). The traditional and hitherto mainly employed approach (GGL hereafter) is to correlate the position of one lens with the shear of one source galaxy.

Schneider & Watts (2005, SW05 hereafter) advanced the traditional GGL by considering a new set of three-point correlation functions that either involves two lenses and one source ("correlator $\mathcal{G}$") or two sources and one lens ("correlator $G_\pm$"). Both correlators are tools to directly study higher-order correlations between galaxies and the surrounding matter field. In the literature, this technique is termed 3rd-order galaxy-galaxy lensing or galaxy-galaxy-galaxy lensing (G3L). There are alternative but mathematically equivalent ways to express these statistics, e.g., the aperture statistics $\langle \mathcal{N}^2 M_{\rm ap}\rangle$ and $\langle \mathcal{N} M_{\rm ap}^2\rangle$ instead of the three-point correlation functions $G_\pm$ and $\mathcal{G}$ (SW05, Simon et al. 2008). In practical measurements usually the aperture statistics are preferred, as they automatically remove unconnected 2nd-order contributions in estimators of the statistics and allow one to separate E-modes

Table 1. List of symbols used in the paper and their meaning.

Symbol	Meaning	Flag	Symbol	Meaning	Flag
$\boldsymbol{\theta}$	position on the sky	C	$P_\alpha(\alpha)$	p.d.f. of internal halo parameters	R
θ	modulus of $\boldsymbol{\theta}$	R	$\boldsymbol{\theta}_i^{\rm h}$	centre position of ith halo	C
$\boldsymbol{\theta}_{ij}$	difference vector $\boldsymbol{\theta}_i - \boldsymbol{\theta}_j$	C	$\overline{\gamma}_{\rm h}(\boldsymbol{\theta})$	mean Cartesian halo shear profile	C
θ_{ij}	modulus of $\boldsymbol{\theta}_{ij}$	R	$\overline{\gamma}_{\rm t,h}(\vartheta)$	mean tangential halo shear profile	R
$\delta_{\rm D}^{(2)}(\boldsymbol{\theta})$	2D Dirac delta function	R	$\overline{\gamma}_{\rm t}(\vartheta)$	mean tangential shear (GGL)	R
$\gamma_{\rm c}(\boldsymbol{\theta})$	Cartesian shear at $\boldsymbol{\theta}$	C	$\delta\gamma_{\rm h}(\boldsymbol{\theta};\boldsymbol{\alpha}_i)$	fluctuation of ith halo shear profile about $\overline{\gamma}_{\rm h}(\boldsymbol{\theta})$	C
$\gamma(\boldsymbol{\theta};\varphi)$	shear at $\boldsymbol{\theta}$ rotated by φ	C	$n_{\rm g}(\boldsymbol{\theta})$	lens number density (on sky)	R
$\gamma_{\rm t}(\boldsymbol{\theta})$	tangential shear at $\boldsymbol{\theta}$ relative to direction $\boldsymbol{\theta}$	R	$\bar{n}_{\rm g}$	mean lens number density (on sky)	R
$\gamma_\times(\boldsymbol{\theta})$	cross shear at $\boldsymbol{\theta}$ relative to direction $\boldsymbol{\theta}$	R	$\kappa_{\rm g}(\boldsymbol{\theta})$	lens number density contrast (on sky)	R
$\gamma_{\rm h}(\boldsymbol{\theta};\boldsymbol{\alpha}_i)$	halo shear profile of ith halo	C	$\omega(\vartheta)$	2pt-clustering of lenses (on sky)	R
$\boldsymbol{\alpha}_i$	internal parameters of ith halo	V	$\Omega(\vartheta_1,\vartheta_2,\vartheta_3)$	3pt-clustering of lenses (on sky)	R

Notes. The flag denotes a real number for "R", a complex number for "C", or vector of numbers for "V".

from B-modes or parity modes, of which the latter two cannot be generated by gravitational lensing as leading order effect. In this paper, we focus on the E-modes in the correlators $\mathcal{G}$ and $G_\pm$.

G3L has already been measured in contemporary lensing surveys, such as the Red-Sequence Cluster Survey (Simon et al. 2008), and will therefore presumably be routinely measured with ongoing surveys such as KiDS[1], Pan-STARRS[2], DES[3], or in the future surveys Euclid[4] and LSST[5]. The prospects of learning more on the galaxy-matter relation or new observational tests for theoretical galaxy models (e.g. Weinberg et al. 2004; Bower et al. 2006; De Lucia et al. 2007) with G3L are thus quite promising.

The main obstacle for exploiting the new G3L statistics is their physical interpretation. It is clear from the definition that $\mathcal{G}$ quantifies the shear signal (or projected matter density) in excess of purely randomly distributed lenses, picking up only signal from clustered lens pairs (e.g., Johnston 2006), and that $G_\pm$ is a two-point correlation function of shear associated with matter physically close to lenses. It is unclear, however, what physical information this translates to and what new feature may be contained in G3L that may be missing or is degenerate in traditional GGL. To elucidate these new statistics and to pave the way for new applications of G3L, we conceive here a simplistic model for the distribution of lenses and matter: the ILM. Then G3L is flashed out in the light of this model. For the definition of quantities relevant for weak gravitational lensing, we refer the reader to Bartelmann & Schneider (2001). The mathematical machinery of a halo model expansion devised in the calculations is very similar to Scherrer & Bertschinger (1991), although used in a different physical context.

The structure of the paper lays out as follows. Section 2 introduces our model and derives the tangential shear about a lens, the GGL signal, expected from this description. Section 3 moves on to calculate the lens-lens-shear or $\mathcal{G}$ correlator for this specific scenario. Section 4 does the same for the lens-lens-shear or $G_\pm$ correlator. The final Sect. 5 summarises the main conclusions drawn in the preceding sections. In the following sections, we are introducing a number of symbols that are listed in Table 1 for clarity.

2. The isolated lens model and galaxy-galaxy lensing

Here we lay out a simple model for the distribution of matter and galaxies inside it. This model is founded on the assumption that lenses are embedded inside a matter halo that generates the shear profile $\gamma_{\rm h}(\boldsymbol{\theta};\boldsymbol{\alpha})$ acting upon a background source, where $\boldsymbol{\theta}$ is the separation vector from the centroid of the galaxy, and $\boldsymbol{\alpha}$ denotes a set of intrinsic halo parameters that control the matter density profile of the halo. Importantly, the intrinsic parameters are statistically independent of the intrinsic halo parameters of any other halo or the separations of other lenses. We hence coin lenses and their host haloes in this scenario "isolated". In this sense, this is a very crude halo model representation (Cooray & Sheth 2002) of the lens and matter distribution, assuming for simplicity that every halo is occupied by exactly one (lens) galaxy. Notice that matter which is statistically independent of the lenses does not need to be accounted for, as this would not contribute to a galaxy-matter cross-correlation function, although it certainly would affect the noise in a measurement.

In the following, 2D positions on the flat sky are, for convenience, denoted by complex numbers $\boldsymbol{\theta} = \theta_1 + {\rm i}\theta_2$ where θ_1 (θ_2) is the position in direction of the $x(y)$-axis. By $\theta = |\boldsymbol{\theta}| = \sqrt{\boldsymbol{\theta}\boldsymbol{\theta}^*}$ we denote the modulus of $\boldsymbol{\theta}$. Likewise the Cartesian shear 2-spinor $\gamma_{\rm c} = \gamma_1 + {\rm i}\gamma_2$ is denoted as complex number. We define the tangential, $\gamma_{\rm t}$, and cross, $\gamma_\times$, shear of $\gamma_{\rm c}(\boldsymbol{\theta})$ relative to the origin by

$$\gamma(\boldsymbol{\theta};\varphi) := \gamma_{\rm t}(\boldsymbol{\theta}) + {\rm i}\gamma_\times(\boldsymbol{\theta}) = -{\rm e}^{-2{\rm i}\varphi}\gamma_{\rm c}(\boldsymbol{\theta}), \tag{1}$$

where φ is the polar angle of $\boldsymbol{\theta}$.

[1] http://www.astro-wise.org/projects/KIDS/
[2] http://www.cfht.hawaii.edu/Science/CFHLS/
[3] http://www.darkenergysurvey.org
[4] http://sci.esa.int/euclid, see also Laureijs et al. (2011).
[5] http://www.lsst.org/

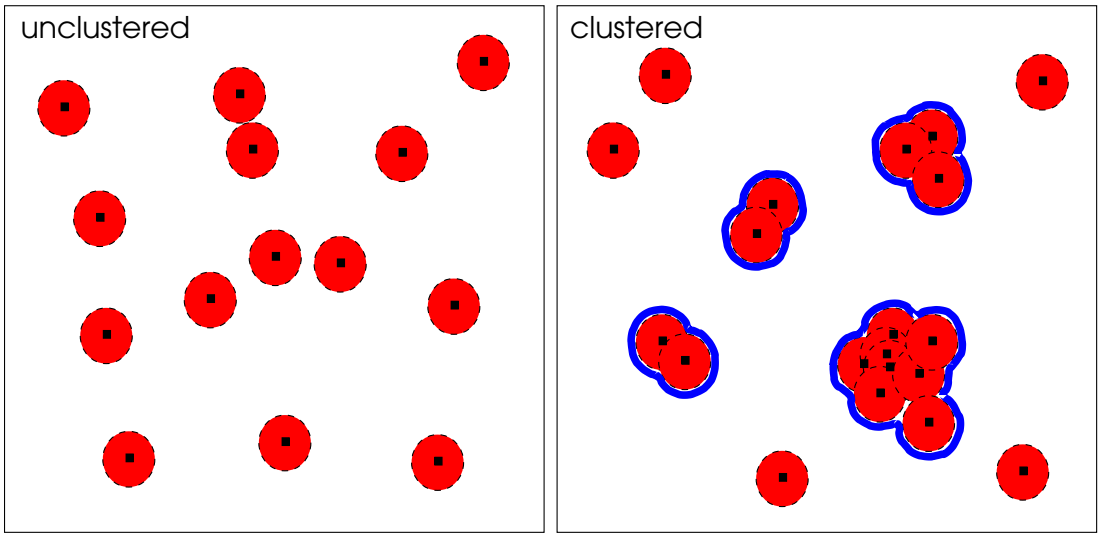

Fig. 1. Illustration of the isolated lens model. Galaxies are depicted by black pixels, their matter haloes as red disks. For simplicity all haloes are identical in this visualisation. *Left panel*: lenses are distributed randomly on the sky. *Right panel*: lenses cluster to produce clumps with a common matter envelope, yet still described as sums of individual haloes. On the statistical level, this clumping is quantified by non-vanishing 2nd-order and 33d-order correlation functions ω and Ω, respectively.

2.1. Isolated lens model

Within the isolated lens model (ILM), the number density distribution of lenses on the (flat) sky with area A is

$$n_{\rm g}(\boldsymbol{\theta}) = \sum_{i=1}^{N_{\rm d}} \delta_{\rm D}^{(2)}(\boldsymbol{\theta} - \boldsymbol{\theta}_i^{\rm h}), \tag{2}$$

where $\delta_{\rm D}^{(2)}(\boldsymbol{\theta})$ is the Dirac delta function, and the resulting shear field is

$$\gamma_{\rm c}(\boldsymbol{\theta}) = \sum_{i=1}^{N_{\rm d}} \gamma_{\rm h}\left(\boldsymbol{\theta} - \boldsymbol{\theta}_i^{\rm h}; \boldsymbol{\alpha}_i\right), \tag{3}$$

sticking a shear profile to every of the $N_{\rm d}$ lens position $\boldsymbol{\theta}_i^{\rm h}$. The shear profile is directly related to the projected matter density about the lens. In the following we will use the lens number density contrast

$$\kappa_{\rm g}(\boldsymbol{\theta}) := \frac{n_{\rm g}(\boldsymbol{\theta})}{\overline{n}_{\rm g}} - 1, \tag{4}$$

where $\overline{n}_{\rm g} := N_{\rm d}/A$ is the mean number density of lenses within the area A. For the 2nd-order angular clustering correlation function of lenses on the sky (e.g. Peebles 1980), we employ the function

$$\omega\left(|\boldsymbol{\theta}_{12}|\right) = \left\langle \kappa_{\rm g}(\boldsymbol{\theta}_1)\kappa_{\rm g}(\boldsymbol{\theta}_2)\right\rangle \tag{5}$$

with $\boldsymbol{\theta}_{ij} := \boldsymbol{\theta}_i - \boldsymbol{\theta}_j$ being the separation vector of two positions. A value $\omega(\theta_{12}) > 0$ expresses an excess of galaxy pairs at separation θ_{12} compared to a purely random distribution.

The ILM is a more general description than may appear at first sight: Galaxy clumps with joint matter envelopes ("galaxy clusters") are not explicitly excluded, although every individual halo does host only one lens. To form matter haloes of whole clusters, we can always stick together and overlap matter haloes, changing the clustering correlation functions in consequence. The difference between the left and right panel of Fig. 1 lies therefore in the choice of the clustering correlation functions, which will enter the following calculations. Hence, the ILM expands larger matter haloes as sums of individual matter haloes of *clustered* galaxies. Crucially, however, the ILM is incapable to implement clumps of N galaxies that contain on average more mass than N isolated galaxies; the mean matter-to-lens-number ratio has to be constant throughout. To form a clump with a higher mass-to-lens number ratio would require to increase the mass of all individual haloes simultaneously, i.e., to change the internal halo parameters of all lenses inside the clump in a similar fashion. This is not allowed, except by chance, however, since internal parameters are statistically independent. A generalisation of the ILM in this direction could be achieved in a full-scale halo model with matter haloes hosting more than one galaxy. Note that the luminosity of a lens can also be seen as an internal parameter. Therefore, a constant mass-to-lens number ratio plus statistical independence of internal parameters amounts also to a constant mass-to-light ratio of all clumps in the model.

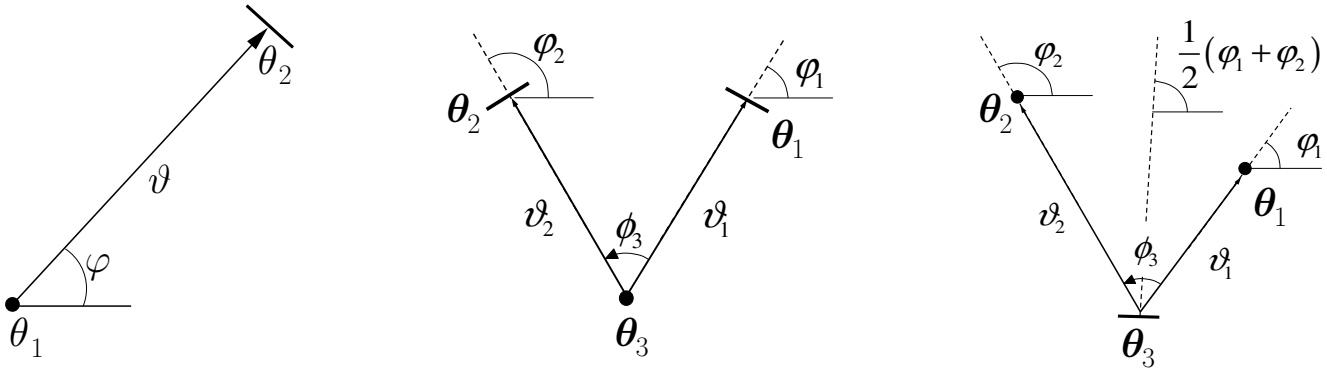

Fig. 2. *Left panel*: illustration of the parametrisation of the GGL correlator $\overline{\gamma}_{\rm t}(\vartheta)$. The lens is located at $\boldsymbol{\theta}_1$, the source is at $\boldsymbol{\theta}_2$. *Middle and right panel*: illustration of the parametrisation of the G3L three-point correlators $\widetilde{G}_{\pm}(\vartheta_1, \vartheta_2, \phi_3)$ (*middle*), and the galaxy-galaxy-shear correlation, $\widetilde{\mathcal{G}}(\vartheta_1, \vartheta_2, \phi_3)$ (*right*). The figures are copied from SW05.

2.2. Galaxy-galaxy lensing

Before we embark on 3rd-order statistics, we start with the more familiar 2nd-order GGL (Bartelmann & Schneider 2001). These statistics are the mean tangential shear $\overline{\gamma}_{\rm t}$ about a lens at separation $\vartheta = |\boldsymbol{\theta}_2 - \boldsymbol{\theta}_1|$ (Fig. 2), defined by the correlator

$$\Big\langle n_{\rm g}(\boldsymbol{\theta}_1)\gamma_{\rm c}(\boldsymbol{\theta}_2)\Big\rangle = -{\rm e}^{+2{\rm i}\varphi}\bar{n}_{\rm g}\left(\Big\langle\kappa_{\rm g}(\boldsymbol{\theta}_1)\gamma(\boldsymbol{\theta}_2;\varphi)\Big\rangle + \underbrace{\Big\langle\gamma(\boldsymbol{\theta}_2;\varphi)\Big\rangle}_{=0}\right) = -{\rm e}^{+2{\rm i}\varphi}\bar{n}_{\rm g}\,\overline{\gamma}_{\rm t}(\vartheta). \tag{6}$$

Owing to isotropy, the mean tangential shear $\overline{\gamma}_{\rm t}$ is only a function of separation ϑ and independent of the polar angle φ. The bracket $\langle\ldots\rangle$ denotes the ensemble average over lens number densities and shear configurations. The underbraced term has to vanish due to the statistical isotropy and homogeneity.

As lens number densities and shear configurations are expanded in terms of haloes in the ILM, we consider the correlator as ensemble average over all possible lens positions and internal halo parameters,

$$\begin{aligned}\Big\langle n_{\rm g}(\boldsymbol{\theta}_1)\gamma_{\rm c}(\boldsymbol{\theta}_2)\Big\rangle &= \Big\langle\sum_{i,j=1}^{N_{\rm d}}\delta_{\rm D}^{(2)}(\boldsymbol{\theta}_1-\boldsymbol{\theta}_i^{\rm h})\gamma_{\rm h}(\boldsymbol{\theta}_2-\boldsymbol{\theta}_j^{\rm h};\boldsymbol{\alpha}_j)\Big\rangle\\ &= \underbrace{\sum_{i=1}^{N_{\rm d}}\Big\langle\delta_{\rm D}^{(2)}(\boldsymbol{\theta}_1-\boldsymbol{\theta}_i^{\rm h})\gamma_{\rm h}(\boldsymbol{\theta}_2-\boldsymbol{\theta}_i^{\rm h};\boldsymbol{\alpha}_i)\Big\rangle_i}_{\rm one-halo}\\ &\quad+\underbrace{\sum_{i\neq j=1}^{N_{\rm d}}\Big\langle\delta_{\rm D}^{(2)}(\boldsymbol{\theta}_1-\boldsymbol{\theta}_i^{\rm h})\gamma_{\rm h}(\boldsymbol{\theta}_2-\boldsymbol{\theta}_j^{\rm h};\boldsymbol{\alpha}_j)\Big\rangle_{i,j}}_{\rm two-halo},\end{aligned} \tag{7}$$

which splits into two separate sums with ensemble averages over all halo parameters of one halo (one-halo term)

$$\Big\langle\ldots\Big\rangle_i := \frac{1}{A}\int{\rm d}^2\theta_i^{\rm h}\,\Big\langle\ldots\Big\rangle_{\boldsymbol{\alpha}_i} \tag{8}$$

or two haloes (two-halo term)

$$\Big\langle\ldots\Big\rangle_{i,j} := \frac{1}{A^2}\int{\rm d}^2\theta_i^{\rm h}{\rm d}^2\theta_j^{\rm h}\,\Big(1+\omega(|\boldsymbol{\theta}_i^{\rm h}-\boldsymbol{\theta}_j^{\rm h}|)\Big)\Big\langle\ldots\Big\rangle_{\boldsymbol{\alpha}_i,\boldsymbol{\alpha}_j}. \tag{9}$$

The statistical independence of halo positions $\boldsymbol{\theta}_i^{\rm h}$ and internal halo parameters $\boldsymbol{\alpha}_i$ is explicitly used here; $\langle\ldots\rangle_{\boldsymbol{\alpha}_i}$ and $\langle\ldots\rangle_{\boldsymbol{\alpha}_i,\boldsymbol{\alpha}_j}$ are the averages over internal halo parameters of a single halo or jointly for two haloes, respectively. For the latter, we stress again that we will assume statistical independence of $\boldsymbol{\alpha}_i$ and $\boldsymbol{\alpha}_j$.

In the following, we will need the average halo shear profile

$$\overline{\gamma}_{\rm h}(\boldsymbol{\theta}) := \Big\langle\gamma_{\rm h}(\boldsymbol{\theta};\boldsymbol{\alpha})\Big\rangle_{\boldsymbol{\alpha}} = \int{\rm d}\alpha\,P_\alpha(\boldsymbol{\alpha})\gamma_{\rm h}(\boldsymbol{\theta};\boldsymbol{\alpha}) = -{\rm e}^{+2{\rm i}\varphi}\,\overline{\gamma}_{\rm t,h}(\theta), \tag{10}$$

$P_\alpha(\boldsymbol{\alpha})$ is the probability density distribution function (p.d.f.) of the internal halo parameters $\boldsymbol{\alpha}$. The tangential halo shear profile $\overline{\gamma}_{\rm t,h}$ is not to be confused with $\overline{\gamma}_{\rm t}$ in Eq. (6) that describes the total mean tangential shear about a lens including contributions from the

lens halo and haloes of clustering neighbouring lenses. Due to rotational symmetry, the average profile $\overline{\gamma}_\mathrm{h}$ has a vanishing cross shear component, for which reason we can express it in terms of the tangential halo shear function $\overline{\gamma}_\mathrm{t,h}(\theta)$, which is only a function of the separation θ.

Utilising this definition, we arrive for the GGL correlator at

$$\begin{aligned}\left\langle n_\mathrm{g}(\boldsymbol{\theta}_1)\gamma_\mathrm{c}(\boldsymbol{\theta}_2)\right\rangle &= \sum_{i=1}^{N_\mathrm{d}}\frac{1}{A}\left\langle\gamma_\mathrm{h}(\boldsymbol{\theta}_{21};\boldsymbol{\alpha})\right\rangle_{\boldsymbol{\alpha}} + \sum_{i\neq j=1}^{N_\mathrm{d}}\frac{1}{A^2}\int \mathrm{d}^2\theta'\,[1+\omega(|\boldsymbol{\theta}'-\boldsymbol{\theta}_{21}|)]\left\langle\gamma_\mathrm{h}(\boldsymbol{\theta}';\boldsymbol{\alpha})\right\rangle_{\boldsymbol{\alpha}} \\ &\approx \bar{n}_\mathrm{g}\overline{\gamma}_\mathrm{h}(\boldsymbol{\theta}_{21}) + \bar{n}_\mathrm{g}^2\int \mathrm{d}^2\theta'\,\omega(|\boldsymbol{\theta}'-\boldsymbol{\theta}_{21}|)\overline{\gamma}_\mathrm{h}(\boldsymbol{\theta}') + \underbrace{\bar{n}_\mathrm{g}^2\int \mathrm{d}^2\theta'\overline{\gamma}_\mathrm{h}(\boldsymbol{\theta}')}_{=0}.\end{aligned} \tag{11}$$

The underbraced term must vanish due to radial symmetry. Inside the sums all terms become independent of individual lens positions $\boldsymbol{\theta}_i^\mathrm{h}$ and halo parameters $\boldsymbol{\alpha}_i$ due to the averaging. The last step assumes that the number of haloes is large, i.e., $N_\mathrm{d} \gg 1$, in particular $N_\mathrm{d}(N_\mathrm{d}-1) \approx N_\mathrm{d}^2$. This will also be assumed for all following calculations.

Employing (6) and (10), we finally find

$$\overline{\gamma}_\mathrm{t}(\vartheta) = \overline{\gamma}_\mathrm{t,h}(\vartheta) + \bar{n}_\mathrm{g}\int \mathrm{d}\theta'\theta'\mathrm{d}\varphi'\,\mathrm{e}^{2\mathrm{i}(\varphi'-\varphi)}\omega(\Psi)\,\overline{\gamma}_\mathrm{t,h}(\theta') = \overline{\gamma}_\mathrm{t,h}(\vartheta) + \bar{n}_\mathrm{g}\int_0^\infty \mathrm{d}\theta\,\theta\,\overline{\gamma}_\mathrm{t,h}(\theta)\int_0^{2\pi}\mathrm{d}\varphi\cos(2\varphi)\,\omega(\Psi) \tag{12}$$

with the expression

$$\Psi := \sqrt{\theta^2+\vartheta^2-2\theta\vartheta\cos\varphi}. \tag{13}$$

The last step in (12) exploits that $\omega(\theta)$ has vanishing imaginary part. In the specific ILM description, the average shear is expanded in terms of two components: the first term in Eq. (12) is the one-halo term, dominating at small separations, whereas the second term is the two-halo term due to the clustering of haloes. Importantly, GGL is only sensitive to the average lens halo $\overline{\gamma}_\mathrm{h}(\boldsymbol{\theta})$ but insensitive to deviations of $\gamma_\mathrm{h}(\boldsymbol{\theta};\boldsymbol{\alpha})$ from $\overline{\gamma}_\mathrm{h}(\boldsymbol{\theta})$ in the actual halo population, which are explicitly allowed within the ILM.

3. Lens-lens-shear correlator

We now turn to G3L, starting with the constellation of two lenses and one source as depicted in the right panel of Fig. 2. The correlator considers a cross-correlation between lens number densities at two positions $\boldsymbol{\theta}_1$ and $\boldsymbol{\theta}_2$ and the shear at $\boldsymbol{\theta}_3$,

$$\left\langle n_\mathrm{g}(\boldsymbol{\theta}_1)n_\mathrm{g}(\boldsymbol{\theta}_2)\gamma_\mathrm{c}(\boldsymbol{\theta}_3)\right\rangle = -\bar{n}_\mathrm{g}^2\mathrm{e}^{+\mathrm{i}(\varphi_1+\varphi_2)}\,\widetilde{\mathcal{G}}(\vartheta_1,\vartheta_2,\phi_3). \tag{14}$$

Statistical homogeneity and isotropy implies that we can extract a correlation function $\tilde{\mathcal{G}}$ from the correlator that is solely a function of lens and source separations, ϑ_1 and ϑ_2, and the opening angle ϕ_3. This function is split into an unconnected, $\widetilde{\mathcal{G}}_\mathrm{nc}$, and a connected part

$$\mathcal{G}(\vartheta_1,\vartheta_2,\phi_3) = \left\langle\kappa_\mathrm{g}(\boldsymbol{\theta}_1)\kappa_\mathrm{g}(\boldsymbol{\theta}_2)\gamma\left(\boldsymbol{\theta}_3;\frac{\varphi_1+\varphi_2}{2}\right)\right\rangle = \widetilde{\mathcal{G}}(\vartheta_1,\vartheta_2,\phi_3) - \widetilde{\mathcal{G}}_\mathrm{nc}(\vartheta_1,\vartheta_2,\phi_3). \tag{15}$$

The connected part vanishes for unclustered lenses, while the unconnected part can be shown to be generally (SW05)

$$\widetilde{\mathcal{G}}_\mathrm{nc}(\vartheta_1,\vartheta_2,\phi_3) := \mathrm{e}^{-\mathrm{i}\phi_3}\overline{\gamma}_\mathrm{t}(\vartheta_1) + \mathrm{e}^{+\mathrm{i}\phi_3}\overline{\gamma}_\mathrm{t}(\vartheta_2), \tag{16}$$

which is just the sum of the GGL shear profile around each lens. Therefore, $\mathcal{G}$ encodes the shear in excess of what is expected from unclustered lenses with the average shear profile $\overline{\gamma}_\mathrm{t}$ around them, or: it quantifies the shear signal about *clustered* lens pairs. Note that the unconnected terms do not contribute to the aperture statistics $\langle\mathcal{N}^2 M_\mathrm{ap}\rangle$ and are thus not the primary quantity measured with G3L.

3.1. Derivation

For $\mathcal{G}$ within the ILM, we need to evaluate the connected terms of the correlator $\langle n_\mathrm{g}(\boldsymbol{\theta}_1)n_\mathrm{g}(\boldsymbol{\theta}_2)\gamma_\mathrm{c}(\boldsymbol{\theta}_3)\rangle$ with the model specifics Eqs. (2) and (3),

$$\begin{aligned}\left\langle n_\mathrm{g}(\boldsymbol{\theta}_1)n_\mathrm{g}(\boldsymbol{\theta}_2)\gamma_\mathrm{c}(\boldsymbol{\theta}_3)\right\rangle &= \left\langle\sum_{i,j,k=1}^{N_\mathrm{d}}\delta_\mathrm{D}^{(2)}(\boldsymbol{\theta}_1-\boldsymbol{\theta}_i^\mathrm{h})\delta_\mathrm{D}^{(2)}(\boldsymbol{\theta}_2-\boldsymbol{\theta}_j^\mathrm{h})\gamma_\mathrm{h}(\boldsymbol{\theta}_3-\boldsymbol{\theta}_k^\mathrm{h};\boldsymbol{\alpha}_k)\right\rangle = \\ &\underbrace{\sum_{i=1}^{N_\mathrm{d}}\left\langle\delta_\mathrm{D}^{(2)}(\boldsymbol{\theta}_1-\boldsymbol{\theta}_i^\mathrm{h})\delta_\mathrm{D}^{(2)}(\boldsymbol{\theta}_2-\boldsymbol{\theta}_i^\mathrm{h})\gamma_\mathrm{h}(\boldsymbol{\theta}_3-\boldsymbol{\theta}_i^\mathrm{h};\boldsymbol{\alpha}_i)\right\rangle_i}_{\text{one-halo}} + \underbrace{\sum_{i\neq j=1}^{N_\mathrm{d}}\left\langle\delta_\mathrm{D}^{(2)}(\boldsymbol{\theta}_1-\boldsymbol{\theta}_i^\mathrm{h})\delta_\mathrm{D}^{(2)}(\boldsymbol{\theta}_2-\boldsymbol{\theta}_j^\mathrm{h})\gamma_\mathrm{h}(\boldsymbol{\theta}_3-\boldsymbol{\theta}_i^\mathrm{h};\boldsymbol{\alpha}_i)\right\rangle_{i,j} + \texttt{(2 perm.)}}_{\text{two-halo}} \\ &+ \underbrace{\sum_{i\neq j\neq k=1}^{N_\mathrm{d}}\left\langle\delta_\mathrm{D}^{(2)}(\boldsymbol{\theta}_1-\boldsymbol{\theta}_i^\mathrm{h})\delta_\mathrm{D}^{(2)}(\boldsymbol{\theta}_2-\boldsymbol{\theta}_j^\mathrm{h})\gamma_\mathrm{h}(\boldsymbol{\theta}_3-\boldsymbol{\theta}_k^\mathrm{h};\boldsymbol{\alpha}_k)\right\rangle_{i,j,k}}_{\text{three-halo}}\end{aligned} \tag{17}$$

where

$$\left\langle \dots \right\rangle_{i,j,k} := \frac{1}{A^3} \int \mathrm{d}^2\theta_i^{\mathrm{h}} \mathrm{d}^2\theta_j^{\mathrm{h}} \mathrm{d}^2\theta_k^{\mathrm{h}} \, [\underbrace{1 + \omega(\theta_{ij}^{\mathrm{h}}) + \omega(\theta_{ik}^{\mathrm{h}}) + \omega(\theta_{jk}^{\mathrm{h}})}_{\text{unconnected}} + \Omega(\theta_{ik}^{\mathrm{h}}, \theta_{jk}^{\mathrm{h}}, \theta_{ij}^{\mathrm{h}})] \left\langle \dots \right\rangle_{\boldsymbol{\alpha}_i, \boldsymbol{\alpha}_j, \boldsymbol{\alpha}_k} \tag{18}$$

is the ensemble average over three haloes (three-halo term). By

$$\Omega(\theta_{13}, \theta_{23}, \theta_{12}) = \left\langle \kappa_{\mathrm{g}}(\boldsymbol{\theta}_1) \kappa_{\mathrm{g}}(\boldsymbol{\theta}_2) \kappa_{\mathrm{g}}(\boldsymbol{\theta}_3) \right\rangle \tag{19}$$

we denote the (connected) 3rd-order angular clustering correlation function of the lenses that only depends on relative galaxy separations. The sum (17) hence decays into a one-halo term (first sum), two-halo (next sum plus two identical sums apart from permutations of the indices i and j) and the three-halo term (last sum). The one-halo term vanishes for $\boldsymbol{\theta}_1 \neq \boldsymbol{\theta}_2$, i.e., distinct lens positions, owing to the Delta functions. For the connected terms, in the halo correlators $\langle \dots \rangle_{i,j}$ or $\langle \dots \rangle_{i,j,k}$ only the summands with the leading order clustering correlation functions are relevant, i.e., only the terms with Ω in the correlator $\langle \dots \rangle_{i,j,k}$, while terms with ω or 1 are part of the unconnected terms (underbraced). They belong to the unconnected part of the 3rd-order lens clustering. Similarly, in $\langle \dots \rangle_{i,j}$ only terms associated with ω are of relevance, the terms generated by 1, the unconnected part of the 2nd-order lens clustering, will go into $\widetilde{\mathcal{G}}_{\mathrm{nc}}$.

By evaluation of all these ensemble averages one thereby obtains for $\boldsymbol{\theta}_1 \neq \boldsymbol{\theta}_2 \neq \boldsymbol{\theta}_3$

$$\mathcal{G}(\vartheta_1, \vartheta_2, \phi_3) = \mathcal{G}_{2\mathrm{h}}(\vartheta_1, \vartheta_2, \phi_3) + \mathcal{G}_{3\mathrm{h}}(\vartheta_1, \vartheta_2, \phi_3) \tag{20}$$

with the two-halo terms (we utilise the relation $\overline{\gamma}_{\mathrm{h}}(-\boldsymbol{\theta}) = \overline{\gamma}_{\mathrm{h}}(\boldsymbol{\theta})$ following from Eq. (10))

$$\begin{aligned} \mathcal{G}_{2\mathrm{h}}(\vartheta_1, \vartheta_2, \phi_3) &:= -\mathrm{e}^{-\mathrm{i}(\varphi_1+\varphi_2)} \omega(|\boldsymbol{\theta}_1 - \boldsymbol{\theta}_2|) (\overline{\gamma}_{\mathrm{h}}(\boldsymbol{\theta}_3 - \boldsymbol{\theta}_1) + \overline{\gamma}_{\mathrm{h}}(\boldsymbol{\theta}_3 - \boldsymbol{\theta}_2)) \\ &= -\mathrm{e}^{+\mathrm{i}(\varphi_1+\varphi_2)} \omega(\vartheta_2) (- \mathrm{e}^{+2\mathrm{i}\varphi_1} \overline{\gamma}_{\mathrm{t,h}}(\vartheta_1) - \mathrm{e}^{+2\mathrm{i}\varphi_2} \overline{\gamma}_{\mathrm{t,h}}(\vartheta_2)) \\ &= \omega(\vartheta_3) (\mathrm{e}^{-\mathrm{i}\phi_3} \overline{\gamma}_{\mathrm{t,h}}(\vartheta_1) + \mathrm{e}^{+\mathrm{i}\phi_3} \overline{\gamma}_{\mathrm{t,h}}(\vartheta_2)), \end{aligned} \tag{21}$$

the lens-lens separation

$$\vartheta_3 = \sqrt{\vartheta_1^2 + \vartheta_2^2 - 2\vartheta_1\vartheta_2 \cos\phi_3} \tag{22}$$

and the three-halo term

$$\begin{aligned} \mathcal{G}_{3\mathrm{h}}(\vartheta_1, \vartheta_2, \phi_3) &:= -\overline{n}_{\mathrm{g}} \mathrm{e}^{-\mathrm{i}(\varphi_1+\varphi_2)} \int \mathrm{d}^2\theta \, \Omega(|\boldsymbol{\theta}_1 - \boldsymbol{\theta}|, |\boldsymbol{\theta}_2 - \boldsymbol{\theta}|, |\boldsymbol{\theta}_1 - \boldsymbol{\theta}_2|) \overline{\gamma}_{\mathrm{h}}(\boldsymbol{\theta}_3 - \boldsymbol{\theta}) \\ &= -\overline{n}_{\mathrm{g}} \mathrm{e}^{-\mathrm{i}(\varphi_1+\varphi_2)} \int \mathrm{d}^2\theta \, \Omega(|\boldsymbol{\theta}_{13} + \boldsymbol{\theta}|, |\boldsymbol{\theta}_{23} + \boldsymbol{\theta}|, \vartheta_3) \, \overline{\gamma}_{\mathrm{h}}(\boldsymbol{\theta}) \\ &= \overline{n}_{\mathrm{g}} \int \mathrm{d}\theta \, \theta \, \mathrm{d}\varphi \, \Omega(\Upsilon(\vartheta_1, \theta, \varphi - \varphi_1), \Upsilon(\vartheta_2, \theta, \varphi - \varphi_2), \vartheta_3) \, \mathrm{e}^{-\mathrm{i}(\varphi_1+\varphi_2-2\varphi)} \overline{\gamma}_{\mathrm{t,h}}(\theta) \\ &= \overline{n}_{\mathrm{g}} \int \mathrm{d}\theta \, \theta \, \mathrm{d}\varphi \, \Omega(\Upsilon(\vartheta_1, \theta, \varphi + \phi_3), \Upsilon(\vartheta_2, \theta, \varphi), \vartheta_3) \, \mathrm{e}^{+2\mathrm{i}(\phi_3+\varphi)} \overline{\gamma}_{\mathrm{t,h}}(\theta) \\ &= \overline{n}_{\mathrm{g}} \mathrm{e}^{+2\mathrm{i}\phi_3} \int_0^\infty \mathrm{d}\theta \, \theta \, \overline{\gamma}_{\mathrm{t,h}}(\theta) \int_0^{2\pi} \mathrm{d}\varphi \cos(2\varphi) \, \Omega(\Upsilon(\vartheta_1, \theta, \varphi + \phi_3), \Upsilon(\vartheta_2, \theta, \varphi), \vartheta_3), \end{aligned} \tag{23}$$

for which we have introduced the auxiliary function

$$\Upsilon(\theta_1, \theta_2, \phi) := \sqrt{\theta_1^2 + \theta_2^2 + 2\theta_1\theta_2 \cos\phi}. \tag{24}$$

The transformations in (23) use $\phi_3 = \varphi_2 - \varphi_1$ and a change of the integral variables $\varphi \mapsto \varphi + \varphi_2$ and $\boldsymbol{\theta} \mapsto \boldsymbol{\theta} + \boldsymbol{\theta}_3$. The last step utilises that $\Omega(\dots)$ has a vanishing imaginary part.

3.2. Interpretation

In the context of $\mathcal{G}$, we can define a *excess mass* map in the following way. The function $\mathcal{G}$ can, for lens pairs of fixed separation ϑ_3, be mapped as excess shear field at position $\boldsymbol{\theta}_3$ with Cartesian shear value

$$\gamma_{\mathrm{c}}(\boldsymbol{\theta}_3 | \boldsymbol{\theta}_1, \boldsymbol{\theta}_2) = -\frac{\boldsymbol{\theta}_{13}\boldsymbol{\theta}_{23}}{|\boldsymbol{\theta}_{13}||\boldsymbol{\theta}_{23}|} \mathcal{G}(\theta_{13}, \theta_{23}, \phi_3), \tag{25}$$

where ϕ_3 is defined as angle spanned by $\boldsymbol{\theta}_{23}$ and $\boldsymbol{\theta}_{13}$. In this map, we fix the lens positions at $\boldsymbol{\theta}_1 = +\vartheta_3/2$ and $\boldsymbol{\theta}_2 = -\vartheta_3/2$ on the x-axis. This shear map can be converted into a convergence map (e.g. Kaiser & Squires 1993), as for example done in Simon et al. (2008). The excess mass from the two-halo term of the ILM is just the halo mass about each lens at $\boldsymbol{\theta}_1$ and $\boldsymbol{\theta}_2$, weighed with the clustering strength $\omega(\vartheta_3)$ of the pair. This is exactly the mass we would anticipate around a pair of lenses, after one has subtracted

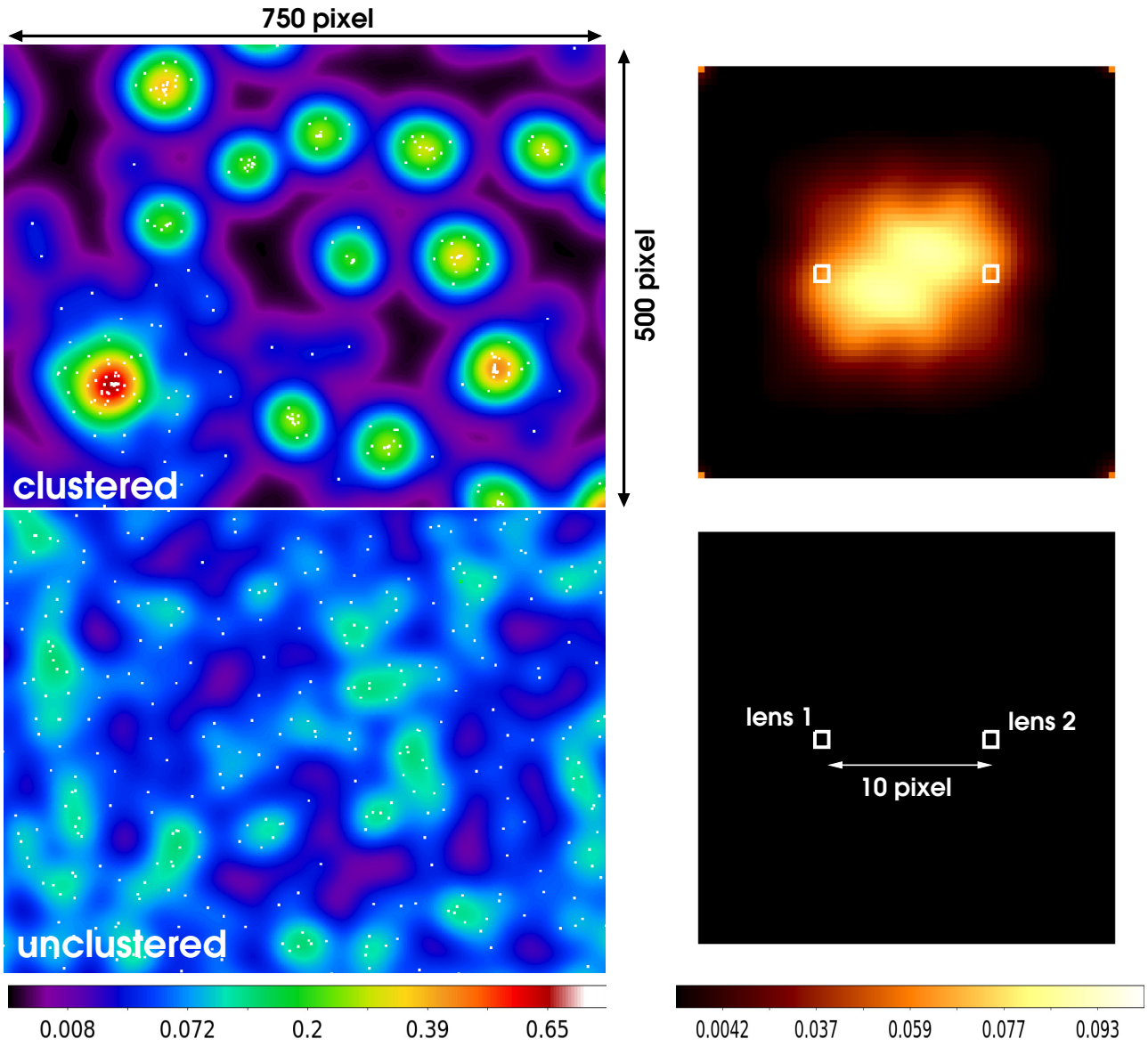

Fig. 3. *Right panels*: excess mass around lens pairs with fixed separation; squares indicate the lens positions inside the maps. *Left panels*: excerpts of the underlying ILM mock data: lenses, shown as little dots, are either clustered (*top left*) or randomly distributed on the sky (*bottom left*). For simplicity, every lens has the same individual matter halo with a Gaussian lensing convergence profile (rms size is 20 pixel) sticked to it. The clustered lens haloes produces the joint matter halo of galaxy clusters in this model. The intensity scale in the *left panels* depicts the combined lensing convergence of all lenses; this is probed as shear by a sample of source galaxies. Note that the angular scale or the shear amplitude are of no particular interest here. The *bottom right panel* is the actual measurement of the *bottom left* scenario with the colour scale of the *top right panel*.

the mass around unclustered pairs (Eq. (21) with $\omega(\vartheta_3) \equiv 1$) and if one ignored the effect of third haloes. The excess mass stemming from a third halo, clustering around the lens pair, is described by the three-halo term.

That the excess shear or mass originates from galaxy clusters can be argued from the ILM (Fig. 3). In the ILM, the excess shear is expressed in terms of the 2nd- and 3rd-order lens clustering correlation functions on the sky. We have no signal, if lenses are unclustered, i.e., $\omega = \Omega = 0$, or simply if we have no galaxy clusters. Unclustered lenses with statistically independent matter haloes cannot produce any excess mass. On the other hand, they still may generate a GGL signal (12) if $\overline{\gamma}_\mathrm{h} \neq 0$. If lenses cluster, i.e., $\omega \neq 0$ or $\Omega \neq 0$, we will get automatically non-vanishing contributions to $\mathcal{G}$. For lens-lens separations comparable or smaller than the typical angular size of a cluster, most lens pairs will inhabit clusters and contribute mostly to the excess mass. Therefore, those pairs probe essentially the matter environment of clusters, provided they are at similar redshift. We do not expect relevant contribution to $\mathcal{G}$ from pairs of lenses with distinct redshifts (apparent pairs), though. Imagine a catalogue of lenses in which all galaxies are clearly separated in radial distance. On the sky, these lenses are (a) unclustered and (b) their matter environments are mutually statistically independent owing to the large physical distances between lenses. This exactly covers the aforementioned situation as reflected in a ILM with vanishing ω and Ω: $\mathcal{G}$ from this lens catalogue vanishes. In comparison with a sample of galaxies all at similar radial distance, a survey with radial spread in the lens distribution will have a larger fraction of apparent pairs, a reduced angular clustering of lenses and hence a overall suppressed amplitude of $\mathcal{G}$. This suppression can be corrected for, if the radial distribution of lenses is specified (Appendix A).

The ILM is only an approximation for the clustering of galaxies and matter since a change of the matter-to-light ratio with size of structures is not possible. Every structure can only be a sum of individual haloes with no correlation to each other. Contrary to GGL this limitation is relevant for G3L, as discussed in the following. We first notice that in comparison with GGL, the lens-lens-shear correlator under ILM assumptions seemingly does not provide any fundamentally new information about the lens-matter connection. To clarify this, the clustering correlation functions (ω, Ω) can be determined by the observable lens angular distribution without exploiting the gravitational lensing effect. Then, by utilising ω and the observed mean tangential shear $\overline{\gamma}_\mathrm{t}$, the average halo shear profile $\overline{\gamma}_\mathrm{h}$ can be constrained from Eq. (12) so that all essential ingredients for predicting $\mathcal{G}$, Eq. (20), are already fixed. In particular, $\mathcal{G}$ appears to be only sensitive to the average halo shear profile as GGL is. Seen this way, G3L can at most complement constraints on the mean shear profile $\overline{\gamma}_\mathrm{h}$. In a scenario more complex than the ILM, however, this differs. Imagine throwing in a few completely different matter haloes into a ILM, hosting several galaxies simultaneously, that cannot be described as sums of individual haloes. Conventional GGL would be unable to detect a difference to a ILM scenario, as we can still use the clustering correlation function ω and the GGL signal $\bar{\gamma}_\mathrm{t}$ with (12) to define an average lens shear profile $\bar{\gamma}_\mathrm{h}$. Therefore the ILM is always, even when falsely presumed, sufficient to consistently describe the GGL signal and the lens clustering. On the other hand, when then combined with $\mathcal{G}$, we would observe inconsistencies, as we fail to correctly explain $\mathcal{G}$ with Eq. (20). In fact, the new haloes with more than one galaxy would produce a one-halo term (Appendix B), which is missing in the ILM description. From this we conclude that $\mathcal{G}$, in combination with GGL, enables us to detect whether a ILM sufficiently explains the data or whether a more advanced description is required.

With the ILM as reference scenario we suggest to construct a test for the applicability of the ILM with the excess signal $\Delta\mathcal{G}$ constructed as follows:

1. use GGL, lens clustering statistics and numbers to obtain the ILM parameter set $(\overline{n}_\mathrm{g}, \omega, \Omega, \bar{\gamma}_\mathrm{h})$ via Eq. (12);
2. define the ILM excess signal by

$$\Delta\mathcal{G}(\vartheta_1, \vartheta_2, \phi_3) := \mathcal{G}(\vartheta_1, \vartheta_2, \phi_3) - \mathcal{G}_\mathrm{2h}(\vartheta_1, \vartheta_2, \phi_3) - \mathcal{G}_\mathrm{3h}(\vartheta_1, \vartheta_2, \phi_3), \tag{26}$$

where the last two terms on the r.h.s. are the two- and three-halo term, Eqs. (21) and (23), from the ILM description.

A vanishing $\Delta\mathcal{G}$ tests the validity of a ILM description for the data or expresses the deviation from it.

4. Lens-lens-shear correlator

Here we predict a measurement for the second G3L correlator $\widetilde{G}_\pm$, given through the correlation of two shears and one lens number density

$$\left\langle \gamma_\mathrm{c}(\boldsymbol{\theta}_1)\gamma_\mathrm{c}^\pm(\boldsymbol{\theta}_2)n_\mathrm{g}(\boldsymbol{\theta}_3)\right\rangle = \bar{n}_\mathrm{g}^{-1}\mathrm{e}^{+2\mathrm{i}(\varphi_1 \mp \varphi_2)}\widetilde{G}_\pm(\vartheta_1, \vartheta_2, \phi_3). \tag{27}$$

The geometry of the correlator is depicted in the middle panel of Fig. 2. Here and in the following equations, a superscript "±" as in $\gamma_\mathrm{c}^\pm$ means γ_c for γ_c^- and γ_c^+ for the complex conjugate γ_c^*. This correlator measures the shear-shear correlations as function of lens separation. As before with $\mathcal{G}$, symmetries demand that the correlator depends only on relative separations and angles given by the triangle defined by lens and source positions. It contains an unconnected part that describes the shear-shear correlations for randomly distributed lenses with no correlation to the shear field, namely (SW05)

$$\widetilde{G}_+^\mathrm{nc}(\vartheta_1, \vartheta_2, \phi_3) := \xi_+(\vartheta_3)\,\mathrm{e}^{+2\mathrm{i}\phi_3}; \widetilde{G}_-^\mathrm{nc}(\vartheta_1, \vartheta_2, \phi_3) := \xi_-(\vartheta_3)\left(\frac{\vartheta_2}{\vartheta_3}\mathrm{e}^{+\mathrm{i}\phi_3/2} - \frac{\vartheta_1}{\vartheta_3}\mathrm{e}^{-\mathrm{i}\phi_3/2}\right)^4; \tag{28}$$

ϑ_3 denotes the source-source separation. As before, the unconnected terms do not contribute to the aperture statistics, here $\langle \mathcal{N} M_\mathrm{ap}^2\rangle$, and are thus of no particular interest for G3L. Subtracting the unconnected terms leaves us with the relevant excess shear-shear correlations about lenses, formally (cf. Eq. (1))

$$G_\pm(\vartheta_1, \vartheta_2, \phi_3) = \left\langle \gamma(\boldsymbol{\theta}_1;\varphi_1)\gamma^\pm(\boldsymbol{\theta}_2;\varphi_2)\kappa_\mathrm{g}(\boldsymbol{\theta}_3)\right\rangle = \widetilde{G}_\pm(\vartheta_1, \vartheta_2, \phi_3) - \widetilde{G}_\pm^\mathrm{nc}(\vartheta_1, \vartheta_2, \phi_3). \tag{29}$$

4.1. Derivation

The evaluation of $G_\pm$ for the ILM boils down to evaluating the connected terms of the triple correlator

$$\begin{aligned}
&\left\langle \gamma_\mathrm{c}(\boldsymbol{\theta}_1)\gamma_\mathrm{c}^\pm(\boldsymbol{\theta}_2)n_\mathrm{g}(\boldsymbol{\theta}_3)\right\rangle = \\
&\underbrace{\sum_i^{N_\mathrm{d}} \left\langle \delta_\mathrm{D}^{(2)}(\boldsymbol{\theta}_3 - \boldsymbol{\theta}_i^\mathrm{h})\gamma_\mathrm{h}(\boldsymbol{\theta}_1 - \boldsymbol{\theta}_i^\mathrm{h};\boldsymbol{\alpha}_i)\gamma_\mathrm{h}^\pm(\boldsymbol{\theta}_2 - \boldsymbol{\theta}_i^\mathrm{h};\boldsymbol{\alpha}_i)\right\rangle_i}_{\text{one-halo}} + \underbrace{\sum_{i\neq j\neq k}^{N_\mathrm{d}} \left\langle \delta_\mathrm{D}^{(2)}(\boldsymbol{\theta}_3 - \boldsymbol{\theta}_i^\mathrm{h})\gamma_\mathrm{h}(\boldsymbol{\theta}_1 - \boldsymbol{\theta}_j^\mathrm{h};\boldsymbol{\alpha}_j)\gamma_\mathrm{h}^\pm(\boldsymbol{\theta}_2 - \boldsymbol{\theta}_k^\mathrm{h};\boldsymbol{\alpha}_k)\right\rangle_{i,j,k}}_{\text{three-halo}} \\
&+ \underbrace{\sum_{i\neq j}^{N_\mathrm{d}} \left\langle \delta_\mathrm{D}^{(2)}(\boldsymbol{\theta}_3 - \boldsymbol{\theta}_i^\mathrm{h})\gamma_\mathrm{h}(\boldsymbol{\theta}_1 - \boldsymbol{\theta}_j^\mathrm{h};\boldsymbol{\alpha}_j)\gamma_\mathrm{h}^\pm(\boldsymbol{\theta}_2 - \boldsymbol{\theta}_i^\mathrm{h};\boldsymbol{\alpha}_i)\right\rangle_{i,j} + \sum_{i\neq j}^{N_\mathrm{d}} \left\langle \delta_\mathrm{D}^{(2)}(\boldsymbol{\theta}_3 - \boldsymbol{\theta}_i^\mathrm{h})\gamma_\mathrm{h}(\boldsymbol{\theta}_1 - \boldsymbol{\theta}_i^\mathrm{h};\boldsymbol{\alpha}_i)\gamma_\mathrm{h}^\pm(\boldsymbol{\theta}_2 - \boldsymbol{\theta}_j^\mathrm{h};\boldsymbol{\alpha}_j)\right\rangle_{i,j}}_{\text{two-halo-2}} \\
&+ \underbrace{\sum_{i\neq j}^{N_\mathrm{d}} \left\langle \delta_\mathrm{D}^{(2)}(\boldsymbol{\theta}_3 - \boldsymbol{\theta}_j^\mathrm{h})\gamma_\mathrm{h}(\boldsymbol{\theta}_1 - \boldsymbol{\theta}_i^\mathrm{h};\boldsymbol{\alpha}_i)\gamma_\mathrm{h}^\pm(\boldsymbol{\theta}_2 - \boldsymbol{\theta}_i^\mathrm{h};\boldsymbol{\alpha}_i)\right\rangle_{i,j}}_{\text{two-halo-1}},
\end{aligned} \tag{30}$$

which now contains a one-halo term, two-halo terms and a three-halo term. We distinguish two categories of two-halo terms: in "two-halo-1", the two shear signals are associated with the same halo, while in "two-halo-2" the shear signals originate from the lens halo and a different neighbouring halo. In analogy to the calculations for the correlator $\mathcal{G}$, only terms associated with the leading order clustering correlation functions in the halo correlators $\langle\ldots\rangle_{i,j}$ (terms with ω) and $\langle\ldots\rangle_{i,j,k}$ (terms with Ω) are of interest for the connected terms; for $\langle\ldots\rangle_i$ all terms are connected. Going through the averages step by step and collecting the connected terms, yields as final result for $\boldsymbol{\theta}_1 \neq \boldsymbol{\theta}_2 \neq \boldsymbol{\theta}_3$

$$G_\pm(\vartheta_1,\vartheta_2,\phi_3) = G_\pm^{\rm 1h}(\vartheta_1,\vartheta_2,\phi_3) + G_\pm^{\rm 2h1}(\vartheta_1,\vartheta_2,\phi_3) + G_\pm^{\rm 2h2}(\vartheta_1,\vartheta_2,\phi_3) + G_\pm^{\rm 3h}(\vartheta_1,\vartheta_2,\phi_3). \tag{31}$$

We start with the three-halo term, which is after performing the integral variable transformations $\boldsymbol{\theta} \mapsto \boldsymbol{\theta} + \boldsymbol{\theta}_3$ and $\boldsymbol{\theta}' \mapsto \boldsymbol{\theta}' + \boldsymbol{\theta}_3$

$$\begin{aligned} G_\pm^{\rm 3h}(\vartheta_1,\vartheta_2,\phi_3) &:= \overline{n}_{\rm g}^2 {\rm e}^{-2{\rm i}(\varphi_1\mp\varphi_2)} \int {\rm d}^2\theta\,{\rm d}^2\theta'\,\Omega(|\boldsymbol{\theta}-\boldsymbol{\theta}_3|,|\boldsymbol{\theta}'-\boldsymbol{\theta}_3|,|\boldsymbol{\theta}-\boldsymbol{\theta}'|)\,\overline{\gamma}_{\rm h}(\boldsymbol{\theta}_1-\boldsymbol{\theta})\overline{\gamma}_{\rm h}^\pm(\boldsymbol{\theta}_2-\boldsymbol{\theta}') \\ &= \overline{n}_{\rm g}^2 {\rm e}^{-2{\rm i}(\varphi_1\mp\varphi_2)} \int {\rm d}^2\theta\,{\rm d}^2\theta'\,\Omega(|\boldsymbol{\theta}|,|\boldsymbol{\theta}'|,|\boldsymbol{\theta}'-\boldsymbol{\theta}|)\,\overline{\gamma}_{\rm h}(\boldsymbol{\theta}_{13}+\boldsymbol{\theta})\overline{\gamma}_{\rm h}^\pm(\boldsymbol{\theta}_{23}+\boldsymbol{\theta}'). \end{aligned} \tag{32}$$

To cast this into a form that no longer explicitly contains any φ_i, we need to do a few more transformations. We first note that for a shifted tangential shear one has

$$\overline{\gamma}_{\rm h}(\boldsymbol{\theta}+\boldsymbol{\theta}') = -\frac{\boldsymbol{\theta}+\boldsymbol{\theta}'}{(\boldsymbol{\theta}+\boldsymbol{\theta}')^*}\,\overline{\gamma}_{\rm t,h}(|\boldsymbol{\theta}+\boldsymbol{\theta}'|) = -{\rm e}^{+2{\rm i}\varphi'}\Delta\left(\frac{\theta}{\theta'},\varphi-\varphi'\right)\overline{\gamma}_{\rm t,h}(\Upsilon(\theta,\theta',\varphi-\varphi')), \tag{33}$$

where

$$\Delta(s,\phi) := \frac{s{\rm e}^{+{\rm i}\phi}+1}{s{\rm e}^{-{\rm i}\phi}+1} = \frac{1+2\,s\cos\phi+s^2\cos(2\phi)-{\rm i}2s(1+s\cos\phi)\sin\phi}{1+s^2+2s\cos\phi}; \Delta^*(s,\phi) = \Delta^{-1}(s,\phi) \tag{34}$$

is an additional phase factor; φ and φ' are the polar angles of $\boldsymbol{\theta}$ and $\boldsymbol{\theta}'$, respectively; Υ is given by the previous Eq. (24). Then this allows us to rewrite the previous equation for $G_\pm^{\rm 3h}$ as

$$\begin{aligned} &G_\pm^{\rm 3h}(\vartheta_1,\vartheta_2,\phi_3) := \\ &\quad \overline{n}_{\rm g}^2 \cancel{{\rm e}^{-2{\rm i}(\varphi_1\mp\varphi_2)}} \int {\rm d}^2\theta\,{\rm d}^2\theta'\,\Omega(|\boldsymbol{\theta}|,|\boldsymbol{\theta}'|,|\boldsymbol{\theta}'-\boldsymbol{\theta}|)\cancel{{\rm e}^{2{\rm i}\varphi_1}}\Delta\left(\frac{\theta}{\vartheta_1},\varphi-\varphi_1\right)\overline{\gamma}_{\rm t,h}(|\boldsymbol{\theta}_{13}+\boldsymbol{\theta}|)\cancel{{\rm e}^{\mp 2{\rm i}\varphi_2}}\Delta^\pm\left(\frac{\theta'}{\vartheta_2},\varphi'-\varphi_2\right)\overline{\gamma}_{\rm t,h}(|\boldsymbol{\theta}_{23}+\boldsymbol{\theta}'|) \\ &= \overline{n}_{\rm g}^2 \int {\rm d}\theta\,\theta\,{\rm d}\theta'\theta'\,{\rm d}\varphi\,{\rm d}\varphi'\Delta\left(\frac{\theta}{\vartheta_1},\varphi-\varphi_1\right)\Delta^\pm\left(\frac{\theta}{\vartheta_2},\varphi'-\varphi_2\right)\Omega(\theta,\theta',\Upsilon(\theta,\theta',\varphi'-\varphi))\,\overline{\gamma}_{\rm t,h}(\Upsilon(\vartheta_1,\theta,\varphi-\varphi_1))\,\overline{\gamma}_{\rm t,h}(\Upsilon(\vartheta_2,\theta',\varphi'-\varphi_2)) \\ &= \overline{n}_{\rm g}^2 \int_0^\infty {\rm d}\theta\,\theta\int_0^\infty {\rm d}\theta'\theta'\int_0^{2\pi}{\rm d}\varphi\int_0^{2\pi}{\rm d}\varphi'\Delta\left(\frac{\theta}{\vartheta_1},\varphi\right)\Delta^\pm\left(\frac{\theta}{\vartheta_2},\varphi'\right)\Omega(\theta,\theta',\Upsilon(\theta,\theta',\varphi'-\varphi+\phi_3))\,\overline{\gamma}_{\rm t,h}(\Upsilon(\vartheta_1,\theta,\varphi))\,\overline{\gamma}_{\rm t,h}(\Upsilon(\vartheta_2,\theta',\varphi')). \end{aligned} \tag{35}$$

The (connected) two-halo terms can be split into two sub-groups. One group is insensitive to shape variations of the lens halo, as it only contains the mean halo shear profile $\overline{\gamma}_{\rm h}$,

$$\begin{aligned} G_\pm^{\rm 2h2}(\vartheta_1,\vartheta_2,\phi_3) &:= \overline{n}_{\rm g}{\rm e}^{-2{\rm i}(\varphi_1\mp\varphi_2)} \int {\rm d}^2\theta\,\omega(|\boldsymbol{\theta}_3-\boldsymbol{\theta}|)(\overline{\gamma}_{\rm h}(\boldsymbol{\theta}_1-\boldsymbol{\theta}_3)\overline{\gamma}_{\rm h}^\pm(\boldsymbol{\theta}_2-\boldsymbol{\theta}) + \overline{\gamma}_{\rm h}(\boldsymbol{\theta}_1-\boldsymbol{\theta})\overline{\gamma}_{\rm h}^\pm(\boldsymbol{\theta}_2-\boldsymbol{\theta}_3)) \\ &= \overline{n}_{\rm g}{\rm e}^{-2{\rm i}(\varphi_1\mp\varphi_2)} \int {\rm d}^2\theta\,\omega(\theta)(\overline{\gamma}_{\rm h}(\boldsymbol{\theta}_{13})\overline{\gamma}_{\rm h}^\pm(\boldsymbol{\theta}_{23}+\boldsymbol{\theta}) + \overline{\gamma}_{\rm h}^\pm(\boldsymbol{\theta}_{23})\overline{\gamma}_{\rm h}(\boldsymbol{\theta}_{13}+\boldsymbol{\theta})) \\ &= \bar{n}_{\rm g}\overline{\gamma}_{\rm t,h}(\vartheta_1)\int_0^\infty {\rm d}\theta\,\theta\,\overline{\gamma}_{\rm t,h}(\theta)\int_0^{2\pi}{\rm d}\varphi\cos(2\varphi)\,\omega(\Upsilon(\vartheta_2,\theta,\varphi)) \\ &+ \bar{n}_{\rm g}\overline{\gamma}_{\rm t,h}(\vartheta_2)\int_0^\infty {\rm d}\theta\,\theta\,\overline{\gamma}_{\rm t,h}(\theta)\int_0^{2\pi}{\rm d}\varphi\cos(2\varphi)\,\omega(\Upsilon(\vartheta_1,\theta,\varphi)) \\ &= \overline{\gamma}_{\rm t,h}(\vartheta_1)(\overline{\gamma}_{\rm t}(\vartheta_2)-\overline{\gamma}_{\rm t,h}(\vartheta_2)) + \overline{\gamma}_{\rm t,h}(\vartheta_2)(\overline{\gamma}_{\rm t}(\vartheta_1)-\overline{\gamma}_{\rm t,h}(\vartheta_1)). \end{aligned} \tag{36}$$

The last step exploits the two-halo term of our previous result (12) for GGL. The terms inside the brackets express the excess tangential shear due to haloes clustering around the lens halo. The steps in the calculation of $G_\pm^{\rm 2h2}$ are by and large identical to the steps undertaken in Sect. 2.2.

The remaining terms in (31) are special, as they are indeed sensitive to halo variations, which sets them clearly apart from all aforementioned correlation functions. The (connected) one-halo term is

$$G_\pm^{\rm 1h}(\vartheta_1,\vartheta_2,\phi_3) := {\rm e}^{-2{\rm i}(\varphi_1\mp\varphi_2)}\left\langle\gamma_{\rm h}(\boldsymbol{\theta}_1-\boldsymbol{\theta}_3;\boldsymbol{\alpha})\gamma_{\rm h}^\pm(\boldsymbol{\theta}_2-\boldsymbol{\theta}_3;\boldsymbol{\alpha})\right\rangle_{\boldsymbol{\alpha}} = {\rm e}^{-2{\rm i}(\varphi_1\mp\varphi_2)}\left\langle\gamma_{\rm h}(\boldsymbol{\theta}_{13};\boldsymbol{\alpha})\gamma_{\rm h}^\pm(\boldsymbol{\theta}_{23};\boldsymbol{\alpha})\right\rangle_{\boldsymbol{\alpha}}. \tag{37}$$

If we write the halo shear as sum of the mean shear profile and some fluctuation $\delta\gamma_{\rm h}(\boldsymbol{\theta};\boldsymbol{\alpha})$ about it, i.e.,

$$\gamma_{\rm h}(\boldsymbol{\theta};\boldsymbol{\alpha}) = \overline{\gamma}_{\rm h}(\boldsymbol{\theta}) + \delta\gamma_{\rm h}(\boldsymbol{\theta};\boldsymbol{\alpha}), \tag{38}$$

with $\langle\delta\gamma_\mathrm{h}(\boldsymbol{\theta};\boldsymbol{\alpha})\rangle_{\boldsymbol{\alpha}} = 0$, then the one-halo term becomes

$$\begin{aligned} G_\pm^{1\mathrm{h}}(\vartheta_1,\vartheta_2,\phi_3) &= \mathrm{e}^{-2\mathrm{i}(\varphi_1\mp\varphi_2)}\left(\overline{\gamma}_\mathrm{h}(\boldsymbol{\theta}_{13})\overline{\gamma}_\mathrm{h}^\pm(\boldsymbol{\theta}_{23}) + \left\langle\delta\gamma_\mathrm{h}(\boldsymbol{\theta}_{13};\boldsymbol{\alpha})\delta\gamma_\mathrm{h}^\pm(\boldsymbol{\theta}_{23};\boldsymbol{\alpha})\right\rangle_{\boldsymbol{\alpha}}\right) \\ &= \overline{\gamma}_{\mathrm{t,h}}(\vartheta_1)\overline{\gamma}_{\mathrm{t,h}}(\vartheta_2) + \mathrm{e}^{-2\mathrm{i}(\varphi_1\mp\varphi_2)}\left\langle\delta\gamma_\mathrm{h}(\boldsymbol{\theta}_{13};\boldsymbol{\alpha})\delta\gamma_\mathrm{h}^\pm(\boldsymbol{\theta}_{23};\boldsymbol{\alpha})\right\rangle_{\boldsymbol{\alpha}} \\ &= \overline{\gamma}_{\mathrm{t,h}}(\vartheta_1)\overline{\gamma}_{\mathrm{t,h}}(\vartheta_2) + \left\langle\delta\gamma_{\mathrm{t,h}}(\vartheta_1,\varphi_1;\boldsymbol{\alpha})\delta\gamma_{\mathrm{t,h}}^\pm(\vartheta_2,\varphi_2;\boldsymbol{\alpha})\right\rangle_{\boldsymbol{\alpha}}. \end{aligned} \tag{39}$$

In the last equation, we employed

$$\gamma_{\mathrm{t,h}}(\theta,\varphi;\boldsymbol{\alpha}) := -\mathrm{e}^{-2\mathrm{i}\varphi}\,\gamma_\mathrm{h}(\boldsymbol{\theta};\boldsymbol{\alpha}); \overline{\gamma}_{\mathrm{t,h}}(\theta) = \left\langle\gamma_{\mathrm{t,h}}(\theta,\varphi;\boldsymbol{\alpha})\right\rangle_{\boldsymbol{\alpha}}, \tag{40}$$

where φ is the polar angle of $\boldsymbol{\theta}$; an equivalent definition is employed for the fluctuations $\delta\gamma_{\mathrm{t,h}}$. Owing to statistical isotropy of the shear field, the model halo shear profile $\gamma_\mathrm{h}(\boldsymbol{\theta};\boldsymbol{\alpha})$ has to have a random orientation. Therefore, the correlator in the previous equation must be invariant with respect to any rotation ϕ, or

$$\begin{aligned} \left\langle\delta\gamma_{\mathrm{t,h}}(\vartheta_1,\varphi_1;\boldsymbol{\alpha})\delta\gamma_{\mathrm{t,h}}^\pm(\vartheta_2,\varphi_2;\boldsymbol{\alpha})\right\rangle_{\boldsymbol{\alpha}} &= \frac{1}{2\pi}\int_0^{2\pi}\mathrm{d}\phi\left\langle\delta\gamma_{\mathrm{t,h}}(\vartheta_1,\varphi_1+\phi;\boldsymbol{\alpha})\delta\gamma_{\mathrm{t,h}}^\pm(\vartheta_2,\varphi_2+\phi;\boldsymbol{\alpha})\right\rangle_{\boldsymbol{\alpha}} \\ &= \frac{1}{2\pi}\int_0^{2\pi}\mathrm{d}\phi\left\langle\delta\gamma_{\mathrm{t,h}}(\vartheta_1,\phi+\phi_3;\boldsymbol{\alpha})\delta\gamma_{\mathrm{t,h}}^\pm(\vartheta_2,\phi;\boldsymbol{\alpha})\right\rangle_{\boldsymbol{\alpha}} \\ &=: \overline{\gamma}_{\mathrm{t,h}}(\vartheta_1)\overline{\gamma}_{\mathrm{t,h}}(\vartheta_2)\,\delta G_\pm^{1h}(\vartheta_1,\vartheta_2,\phi_3). \end{aligned} \tag{41}$$

The remaining two-halo term in (31) is similar to the one-halo term, actually an integral over $G_\pm^{1\mathrm{h}}$,

$$\begin{aligned} G_\pm^{2\mathrm{h}1}(\vartheta_1,\vartheta_2,\phi_3) &:= \overline{n}_\mathrm{g}\mathrm{e}^{-2\mathrm{i}(\varphi_1\mp\varphi_2)}\int\mathrm{d}^2\theta\,\omega(|\boldsymbol{\theta}-\boldsymbol{\theta}_3|)\left\langle\gamma_\mathrm{h}(\boldsymbol{\theta}_1-\boldsymbol{\theta};\boldsymbol{\alpha})\gamma_\mathrm{h}^\pm(\boldsymbol{\theta}_2-\boldsymbol{\theta};\boldsymbol{\alpha})\right\rangle_{\boldsymbol{\alpha}} \\ &= \overline{n}_\mathrm{g}\mathrm{e}^{-2\mathrm{i}(\varphi_1\mp\varphi_2)}\int\mathrm{d}^2\theta\,\omega(\theta)\left\langle\gamma_\mathrm{h}(\boldsymbol{\theta}_{13}+\boldsymbol{\theta};\boldsymbol{\alpha})\gamma_\mathrm{h}^\pm(\boldsymbol{\theta}_{23}+\boldsymbol{\theta};\boldsymbol{\alpha})\right\rangle_{\boldsymbol{\alpha}} \\ &= \overline{n}_\mathrm{g}\cancel{\mathrm{e}^{-2\mathrm{i}(\varphi_1\mp\varphi_2)}}\int\mathrm{d}^2\theta\,\omega(\theta)\cancel{\mathrm{e}^{\mp2\mathrm{i}\varphi_1}}\cancel{\mathrm{e}^{\mp2\mathrm{i}\varphi_2}}\Delta\left(\frac{\theta}{\vartheta_1},\varphi-\varphi_1\right)\Delta^\pm\left(\frac{\theta}{\vartheta_2},\varphi-\varphi_2\right)G_\pm^{1\mathrm{h}}(\Upsilon(\vartheta_1,\theta,\varphi-\varphi_1),\Upsilon(\vartheta_2,\theta,\varphi-\varphi_2),\nu) \\ &= \overline{n}_\mathrm{g}\int_0^\infty\mathrm{d}\theta\,\theta\int_0^{2\pi}\mathrm{d}\varphi\,\omega(\theta)\Delta\left(\frac{\theta}{\vartheta_1},\varphi+\phi_3\right)\Delta^\pm\left(\frac{\theta}{\vartheta_2},\varphi\right)G_\pm^{1\mathrm{h}}(\Upsilon(\vartheta_1,\theta,\varphi+\phi_3),\Upsilon(\vartheta_2,\theta,\varphi),\mu), \end{aligned} \tag{42}$$

where the angle ν spanned by $\boldsymbol{\theta}_{23}+\boldsymbol{\theta}$ and $\boldsymbol{\theta}_{13}+\boldsymbol{\theta}$ and the corresponding angle μ for a $\boldsymbol{\theta}$ rotated by φ_2 are implicitly given by

$$\mathrm{e}^{\mathrm{i}\nu} = \frac{\boldsymbol{\theta}_{23}+\boldsymbol{\theta}}{\boldsymbol{\theta}_{13}+\boldsymbol{\theta}}\frac{|\boldsymbol{\theta}_{13}+\boldsymbol{\theta}|}{|\boldsymbol{\theta}_{23}+\boldsymbol{\theta}|} = \frac{\vartheta_2\mathrm{e}^{-\mathrm{i}(\varphi-\varphi_2)}+\theta}{\vartheta_1\mathrm{e}^{-\mathrm{i}(\varphi-\varphi_1)}+\theta}\frac{\Upsilon(\vartheta_1,\theta,\varphi-\varphi_1)}{\Upsilon(\vartheta_2,\theta,\varphi-\varphi_2)}; \mathrm{e}^{\mathrm{i}\mu} = \frac{\vartheta_2\mathrm{e}^{-\mathrm{i}\varphi}+\theta}{\vartheta_1\mathrm{e}^{-\mathrm{i}(\varphi+\phi_3)}+\theta}\frac{\Upsilon(\vartheta_1,\theta,\varphi+\phi_3)}{\Upsilon(\vartheta_2,\theta,\varphi)}. \tag{43}$$

4.2. Interpretation

The resulting $G_\pm$ is the lowest-order galaxy-galaxy lensing correlation function that, at least within the framework of the ILM, is sensitive to variations among shear profiles of haloes. Nevertheless, we also have a $G_\pm$ signal when all halo shear profiles are identical, i.e., $\delta\gamma_{\mathrm{t,h}} = 0$, which is generated by the tangential shear of the lens halo and the excess tangential shear of clustering neighbouring haloes. Only (39) and (42), which both contain the correlator $\delta G^{1\mathrm{h}}$, are affected by a scatter in halo matter profiles. The one-halo term of $G_\pm$ remains unchanged, even if we allow for general correlations between halo parameters $\boldsymbol{\alpha}$ of distinct haloes or for correlations between lens positions and $\boldsymbol{\alpha}$, since a statistical independence of haloes has not been used for this term. Therefore, we expect the behaviour of $G_\pm$ on small angular scales to be described generally by $G_\pm^{1\mathrm{h}}$, not just within the ILM.

In the simplest case that all halo shear profiles are exactly identical, $\gamma_\mathrm{h}(\boldsymbol{\theta};\boldsymbol{\alpha}) = \overline{\gamma}_\mathrm{h}(\boldsymbol{\theta})$, we find

$$G_\pm^{1\mathrm{h}}(\vartheta_1,\vartheta_2,\phi_3) = \overline{\gamma}_{\mathrm{t,h}}(\vartheta_1)\overline{\gamma}_{\mathrm{t,h}}(\vartheta_2); \delta G^{1\mathrm{h}}(\vartheta_1,\vartheta_2,\phi_3) = 0, \tag{44}$$

i.e., the one-halo term has no explicit dependence on the opening angle ϕ_3. Note that $G_+^{1\mathrm{h}}$ and $G_-^{1\mathrm{h}}$ are identical. As illustration of the impact of variance in halo shear profiles, consider a singular isothermal ellipsoid (SIE) profile with ellipticity ϵ_h and random orientation ϕ (Mandelbaum et al. 2006a)

$$\gamma_\mathrm{h}^{\mathrm{sie}}(\boldsymbol{\theta}) \propto -\frac{\mathrm{e}^{+2\mathrm{i}\varphi}}{\theta}\left(1+\frac{\epsilon_\mathrm{h}}{2}\cos(2\varphi+2\phi)\right), \tag{45}$$

φ is the polar angle of $\boldsymbol{\theta}$. The absolute amplitude of the shear profile is not of interest here. The tangential shear profile of the SIE is

$$\gamma_{\mathrm{t,h}}^{\mathrm{sie}}(\theta,\varphi) \propto \frac{1}{\theta}\left(1+\frac{\epsilon_\mathrm{h}}{2}\cos(2\varphi+2\phi)\right). \tag{46}$$

In this case, we find by marginalising over all orientations ϕ,

$$G_{\pm}^{\rm 1h}(\vartheta_1,\vartheta_2,\phi_3) = \frac{1}{2\pi}\int_0^{2\pi} {\rm d}\phi\, \gamma_{\rm t,h}^{\rm sie}(\vartheta_1,\phi_3)\left[\gamma_{\rm t,h}^{\rm sie}(\vartheta_2,0)\right]^{\pm} \propto \overline{\gamma}_{\rm t,h}(\vartheta_1)\overline{\gamma}_{\rm t,h}(\vartheta_2)\left(1+\frac{\epsilon_{\rm h}^2}{8}\cos\left(2\phi_3\right)\right); \overline{\gamma}_{\rm t,h}(\vartheta) \propto \frac{1}{\vartheta}, \tag{47}$$

thus similar to the previous result but now with an additional ϕ_3-dependent term, or

$$\delta G_{\pm}^{\rm 1h}(\vartheta_1,\vartheta_2,\phi_3) = \frac{\epsilon_{\rm h}^2}{8}\cos\left(2\phi_3\right). \tag{48}$$

The result becomes somewhat more complicated for general slopes δ (Appendix C) and will reveal a difference between $G_+^{\rm 1h}$ and $G_-^{\rm 1h}$ when $\delta \neq 1$ (not SIE) and $\epsilon_{\rm h} \neq 0$ (elliptical). Moreover, the correlator (41) will exhibit no ϕ_3-dependence, if the lens haloes are always axially symmetric, even though their radial matter density profile or their mass may scatter as to be expected in reality. Therefore, we conclude that $G_\pm$ may in principle be used to constrain the shape or, more specifically, the mean second-moment of the projected halo matter density profiles. In addition to that, fluctuations $\delta\gamma_{\rm t,h}$ in the halo shear profile due to halo substructure also add to the variance dependent one- and two-halo term of $G_\pm$. As with the foregoing $\mathcal{G}$, it may be useful to define an excess $\Delta G_\pm$, obtained by subtracting off the $G_\pm$-signal as anticipated from the ILM with parameters from lens clustering and GGL. In the ILM regime, the excess signal $\Delta G_\pm$ exactly vanishes, if there is no scatter in the (projected) matter density profiles.

5. Conclusions

In order to gain a better understanding of G3L, we conceived a toy model, the "isolated lens model" (ILM), for the distribution of galaxies and matter about galaxies. In this picture, "isolated" galaxies are surrounded by their own matter envelope (halo). Variations in the halo matter density profile are explicitly allowed, albeit statistically independent to variations of other matter envelopes or to positions of other lenses. Consequently, the matter environment of clusters is herein the superposition of independent haloes produced by clustering galaxies. The average independent matter halo is described by the mean tangential shear around lenses and the clustering of the lenses (GGL), Eq. (12). The foregoing calculations evaluate what would be measured by G3L (Eqs. (20) and (31)) under the ILM assumptions and discuss the results. Here we summarise our main conclusions.

5.1. Excess shear about lens pairs

The lens-lens-shear correlation function $\mathcal{G}$ basically stacks the shear field about clustered lens pairs as opposed to GGL, which stacks the shear field about individual lenses. "Clustered lens pairs" refers to the fact that the connected part of the lens-lens-shear correlator $\mathcal{G}$ does not include the expected shear pattern around pairs formed by randomly distributed lenses[6]. "Excess mass" refers to the convergence map that corresponds to the excess shear of lens pairs. Our conclusions are:

- Unclustered lenses do not generate any $\mathcal{G}$ signal, although they may exhibit a GGL signal. $\mathcal{G}$ is a probe for the matter environment of clusters (or groups), probed by lens pairs inhabiting the cluster.
- Apparent lens pairs formed by lenses well separated in redshift, overall diminish the signal and add noise. The signal-to-noise of $\mathcal{G}$ can thus probably be improved by exploiting lens redshift information and by giving more weight to lenses that are close in redshift. The susceptibility of the $\mathcal{G}$ amplitude as to the radial distribution of lenses can be normalised (Appendix A).
- In the ILM, the excess mass constituents are the haloes about the clustered lens pairs (two-halo term; Eq. (21)) and a third halo clustering about the clustered lens pair (three-halo term; Eq. (23)). In a more elaborate model incorporating haloes hosting more than one galaxy at a time, we expect also one-halo terms adding to the excess mass (Appendix B), especially at small scales.
- If the ILM is a fair description, then $\mathcal{G}$ does not provide any new information on the galaxy-matter connection compared to GGL combined with 2nd-order galaxy clustering. $\mathcal{G}$ can at most complement the information on the mean halo shear profile.
- G3L in combination with GGL and lens clustering can probe whether the matter environments of clusters could be expanded as sums of independent haloes, as in the ILM. In particular, a sum of independent haloes would be unable to change the mass-to-light ratio compared to that of field galaxies.
- Moreover, the ILM can be employed as reference to quantify the deviation $\Delta\mathcal{G}$ from the ILM picture in the real matter distribution around galaxies. This can be devised as practical test for a more advanced halo-model picture that naturally presumes the possibility of genuine joint matter haloes of galaxies that are fundamentally different to sums of matter haloes about isolated lenses. In analogy to $\mathcal{G}$, $\Delta\mathcal{G}$ can be visualised as mass map about lens pairs or as aperture statistics.

5.2. Excess shear-shear correlations about lenses

Unlike GGL and $\mathcal{G}$, which both stack shear about lenses, $G_\pm$ measures the excess shear-shear correlations relative to a lens position. "Excess" means in this context shear-shear correlations in contrast to randomly distributed lenses, which would have a vanishing

[6] Strictly speaking, $\widetilde{\mathcal{G}}$ is not the stacked, average shear field about lens pairs but the average shear pattern *times* the frequency of lens pairs at separation ϑ_3 normalised by the same frequency for randomly distributed lenses, i.e., times the factor $1+\omega(\vartheta_3)$.

GGL or $\mathcal{G}$ signal. In this respect, $G_\pm$ more resembles the shear-shear correlation function $\xi_\pm$ utilised in cosmic shear studies (e.g. Schneider 2006) rather than GGL. Our conclusions are:

- In the ILM, or more generally in a full halo model picture, the excess shear-shear correlations have two basic contributors: (i) the host halo of a lens (one-halo term; Eq. (39)); and (ii) neighbouring haloes clustering about the lens (two-halo terms: Eqs. (42) and (36); three-halo term: Eq. (35)).
- $G_\pm$ is the lowest-order galaxy-galaxy lensing correlation function that is sensitive to variations in the (projected) density profiles of matter around lenses. Traditional GGL and $\mathcal{G}$ are only functions of the mean, stacked shear profiles.
- In particular is $G_\pm$ sensitive to variations due to elliptical haloes with random orientations. Therefore, the correlator is principally sensitive to the shape of matter haloes and could be exploited as such to measure halo shapes without the need of luminous tracers of presumed alignment to the halo. An elliptical halo generates an extra ϕ_3-modulation in $G_\pm$, where ϕ_3 is the opening angle between the two lens-source directions. The one-halo term of $G_\pm$ does not exhibit a ϕ_3-modulation for spherical haloes.
- Halo substructure, i.e., random fluctuations about a smooth halo profile, also contribute to the one- and two-halo term of $G_\pm$. Therefore, $G_\pm$ is in principle also sensitive to halo substructure.
- The one-halo term of $G_\pm$ is unchanged, if we generally allow for statistical dependences of the lens haloes within the framework of a general model. Therefore, the ellipticity and substructure effect will also be present to some extend, if we have strong deviations from the ILM assumptions. However, it is unclear at this point how strong the effects are, even within the ILM, and what possible degeneracies are. We defer a thorough study of these effects to a future paper.

Acknowledgements. This work has been supported by the Deutsche Forschungsgemeinschaft in the framework of the Collaborative Research Center TR33 "The Dark Universe". Patrick Simon also acknowledges supported by the European DUEL Research-Training Network (MRTN-CT-2006-036133).

Appendix A: Normalisation scheme

Let

$$\Sigma_{\rm crit}(\chi_{\rm s},\chi_{\rm d}) := \frac{c^2}{4\pi G a(\chi_{\rm d})}\frac{f_{\rm K}(\chi_{\rm s})}{f_{\rm K}(\chi_{\rm s}-\chi_{\rm d})f_{\rm K}(\chi_{\rm d})};\rho_{\rm crit} := \frac{3H_0^2}{8\pi G} \tag{A.1}$$

be the critical surface matter density for lenses at comoving distance $\chi_{\rm d}$ and sources at $\chi_{\rm s}$, and the critical density of the Universe, respectively; $f_{\rm K}(\chi)$ denotes the angular diameter distance. Using Limber's equation for projecting the 3D bispectrum to the angular 2D bispectrum, SW05 showed for

$$|k|^2 := k_1^2+k_2^2-2k_1k_2\cos\psi; A^2 := k_1^2R_1^2+k_2^2R_2^2-2k_1k_2R_1R_2\cos(\psi_3-\psi); {\rm e}^{2{\rm i}\nu} := \frac{1}{A^2}\left[2k_1k_2R_1R_2+(k_1R_1)^2{\rm e}^{{\rm i}(\phi_3-\psi)}+(k_2R_2)^2{\rm e}^{{\rm i}(\phi_3-\psi)}\right] \tag{A.2}$$

that

$$\mathcal{G}(\vartheta_1,\vartheta_2,\phi_3) = \Omega_{\rm m}\rho_{\rm crit}\int_0^{\chi_{\rm h}}\frac{{\rm d}\chi{\rm d}\chi' p_{\rm b}(\chi')p_{\rm f}(\chi)^2}{\Sigma_{\rm crit}(\chi',\chi)}\int\frac{{\rm d}k_1k_1{\rm d}k_2k_2{\rm d}\Psi}{(2\pi)^3}\underbrace{\frac{\left(k_1{\rm e}^{-{\rm i}\psi/2}+k_2{\rm e}^{+{\rm i}\psi/2}\right)^2}{|k|^2}{\rm e}^{2{\rm i}\nu}J_2(A)}_{=:K(k_1,k_2,R_1,R_2,\psi)}B_{\rm ggm}(k_1,k_2,\psi;\chi); \tag{A.3}$$

$p_{\rm f}(\chi)$ and $p_{\rm b}(\chi)$ are the radial lens and source distribution; $B_{\rm ggm}(k_1,k_2,\psi;\chi)$ is the galaxy-galaxy-matter bispectrum at comoving radial distance χ; the wave numbers k_i are also in comoving units. Note that we here, inside the integral, transformed angular separations ϑ_i to the projected comoving distance at lens plane distance χ, $R_i := f_{\rm K}(\chi)\vartheta_i$. We recast this equation into

$$\begin{aligned}\mathcal{G}(\overline{R}_1,\overline{R}_2,\phi_3) &:= \Omega_{\rm m}\rho_{\rm crit}\int_0^{\chi_{\rm h}}\frac{{\rm d}\chi{\rm d}\chi' p_{\rm b}(\chi')p_{\rm f}(\chi)^2}{\Sigma_{\rm crit}(\chi',\chi)}\times\int\frac{{\rm d}k_1k_1{\rm d}k_2k_2{\rm d}\psi}{(2\pi)^3}K(k_1,k_2,R_1,R_2,\psi)\,B_{\rm ggm}(k_1,k_2,\psi;\chi)\\ &=: \mathcal{G}_0\times\int\frac{{\rm d}k_1k_1{\rm d}k_2k_2{\rm d}\psi}{(2\pi)^3}K(k_1,k_2,R_1,R_2,\psi)\,B_{\rm ggm}(k_1,k_2,\psi;\overline{\chi}_{\rm d})\end{aligned} \tag{A.4}$$

where $B_{\rm ggm}(k_1,k_2,\psi;\overline{\chi}_{\rm d})$ is the bispectrum at effective lens plane distance $\overline{\chi}_{\rm d}$ defined by

$$\int_0^{\chi_{\rm h}}\frac{{\rm d}\chi{\rm d}\chi' p_{\rm b}(\chi')p_{\rm f}(\chi)^2}{\Sigma_{\rm crit}(\chi',\chi)}B_{\rm ggm}(k_1,k_2,\psi;\chi) =: B_{\rm ggm}(k_1,k_2,\psi;\overline{\chi}_{\rm d})\int_0^{\chi_{\rm h}}\frac{{\rm d}\chi{\rm d}\chi' p_{\rm b}(\chi')p_{\rm f}(\chi)^2}{\Sigma_{\rm crit}(\chi',\chi)} = B_{\rm ggm}(k_1,k_2,\psi;\overline{\chi}_{\rm d})\,\mathcal{G}_0, \tag{A.5}$$

and $\overline{R}_i = f_{\rm K}(\overline{\chi}_{\rm d})\vartheta_i$ is the projected comoving distance of angular separation ϑ_i at the effective lens plane distance. Therefore, normalising $\mathcal{G}$ by $\mathcal{G}_0$ corrects the correlator for the amplitude reduction due to lens pairs with lenses at distinct redshifts, encoded in $p_{\rm f}(\chi)$, and removes lensing related quantities, yielding a bispectrum at an effective distance $\overline{\chi}_{\rm d}$ projected onto the lens plane by kernel $K(\ldots)$.

Similarly, we find for the lens-lens-shear correlator

$$G_\pm(\overline{R}_1,\overline{R}_2,\phi_3) = G_{\pm_0}\times\int\frac{{\rm d}k_1k_1{\rm d}k_2k_2{\rm d}\psi}{(2\pi)^3}K_\pm(k_1R_1,k_2R_2,\psi)\,B_{\rm mmg}(k_1,k_2,\psi;\overline{\chi}_{\rm d}) \tag{A.6}$$

with

$$G_{\pm_0} := \Omega_\mathrm{m}^2\rho_\mathrm{crit}^2 \int_0^{\chi_\mathrm{h}} \frac{\mathrm{d}\chi\mathrm{d}\chi' p_\mathrm{b}(\chi')p_\mathrm{f}(\chi)}{\Sigma_\mathrm{crit}(\chi',\chi)^2}; \int_0^{\chi_\mathrm{h}} \frac{\mathrm{d}\chi\mathrm{d}\chi' p_\mathrm{b}(\chi')p_\mathrm{f}(\chi)}{\Sigma_\mathrm{crit}(\chi',\chi)^2} B_\mathrm{mmg}(k_1,k_2,\psi;\chi) =: B_\mathrm{mmg}(k_1,k_2,\psi;\overline{\chi}_\mathrm{d})\,\frac{G_{\pm_0}}{\Omega_\mathrm{m}^2\rho_\mathrm{crit}^2} \tag{A.7}$$

and the integral kernels

$$K_+(k_1R_1,k_2R_2,\psi) := \mathrm{e}^{-2\mathrm{i}(\psi_3-\varphi_2)}J_0(A); K_-(k_1R_1,k_2R_2,\psi) := \mathrm{e}^{+4\mathrm{i}\nu}J_4(A). \tag{A.8}$$

Appendix B: One-halo term for $\mathcal{G}$ in a more complex model

The ILM does not have any one-halo terms for $\mathcal{G}$ since haloes are hosting only one lens at a time. Matter haloes of clusters have to be represented as sums of independent haloes. In a more realistic situation beyond the ILM, we can imagine genuinely new haloes, hosting more than one galaxy, that cannot be expanded as sum of independent haloes. For simplicity, for this new type of haloes we here assume round haloes with shear profile $\overline{\gamma}_\mathrm{h}(\boldsymbol{\theta})$; $\boldsymbol{\theta}=0$ is the centre of the halo. Every halo hosts the same number of N_g galaxies. Galaxies belonging to the ith halo are scattered throughout the halo with a separation $\Delta\boldsymbol{\theta}_{ij}$ relative to the halo centre $\boldsymbol{\theta}_i^\mathrm{h}$. Now the number density of galaxies on the sky and the (relevant) shear field associated with the new halo type are

$$n_\mathrm{g}(\boldsymbol{\theta}) = \sum_{i=1}^{N_\mathrm{h}}\sum_{j=1}^{N_\mathrm{g}} \delta_\mathrm{D}(\boldsymbol{\theta}-\boldsymbol{\theta}_i^\mathrm{h}-\Delta\boldsymbol{\theta}_{ij}); \gamma_\mathrm{c}(\boldsymbol{\theta}) = \sum_{i=1}^{N_\mathrm{h}} \overline{\gamma}_\mathrm{h}(\boldsymbol{\theta}-\boldsymbol{\theta}_i^\mathrm{h}). \tag{B.1}$$

In the following, we will focus on the connected one-halo terms of the lens-lens-shear correlator only,

$$\left\langle n_\mathrm{g}(\boldsymbol{\theta}_1)n_\mathrm{g}(\boldsymbol{\theta}_2)\gamma_\mathrm{c}(\boldsymbol{\theta}_3)\right\rangle = \sum_{i=1}^{N_\mathrm{h}}\sum_{j=1}^{N_\mathrm{d}} \left\langle \delta_\mathrm{D}(\boldsymbol{\theta}_1-\boldsymbol{\theta}_i^\mathrm{h}-\Delta\boldsymbol{\theta}_{ij})\delta_\mathrm{D}(\boldsymbol{\theta}_2-\boldsymbol{\theta}_i^\mathrm{h}-\Delta\boldsymbol{\theta}_{ij})\overline{\gamma}_\mathrm{h}(\boldsymbol{\theta}_3-\boldsymbol{\theta}_i)\right\rangle_{i,j} \tag{B.2}$$

$$+ \sum_{i=1}^{N_\mathrm{h}}\sum_{j\neq k=1}^{N_\mathrm{d}} \left\langle \delta_\mathrm{D}(\boldsymbol{\theta}_1-\boldsymbol{\theta}_i^\mathrm{h}-\Delta\boldsymbol{\theta}_{ij})\delta_\mathrm{D}(\boldsymbol{\theta}_2-\boldsymbol{\theta}_i^\mathrm{h}-\Delta\boldsymbol{\theta}_{ik})\overline{\gamma}_\mathrm{h}(\boldsymbol{\theta}_3-\boldsymbol{\theta}_i)\right\rangle_{i,j,k} \tag{B.3}$$

$$+ \texttt{(2-halo terms)} + \texttt{(3-halo terms)}, \tag{B.4}$$

where we have the ensemble averages

$$\left\langle\ldots\right\rangle_{i,j} := \frac{1}{A}\int \mathrm{d}^2\theta_i\,\mathrm{d}^2\Delta\theta_{ij}\,P_\Delta(|\Delta\boldsymbol{\theta}_{ij}|)[\ldots]; \left\langle\ldots\right\rangle_{i,j,k} := \frac{1}{A}\int \mathrm{d}^2\theta_i\,\mathrm{d}^2\Delta\theta_{ij}\,\mathrm{d}^2\Delta\theta_{ik}\,P_\Delta(|\Delta\boldsymbol{\theta}_{ij}|,|\Delta\boldsymbol{\theta}_{ik}|,|\Delta\boldsymbol{\theta}_{ij}-\Delta\boldsymbol{\theta}_{ik}|)[\ldots]. \tag{B.5}$$

By $P_\Delta(\Delta\theta)$ we denote the p.d.f. of a single relative galaxy position inside a halo, whereas by $P_\Delta(\Delta\theta,\Delta\theta',|\Delta\boldsymbol{\theta}-\Delta\boldsymbol{\theta}'|)$ we denote the joint p.d.f. of two galaxy positions. Owing to isotropy, the former can only be a function of the modulus of $\Delta\boldsymbol{\theta}$, the latter only a function of the relative separations $|\Delta\boldsymbol{\theta}|$, $|\Delta\boldsymbol{\theta}'|$ and $|\Delta\boldsymbol{\theta}-\Delta\boldsymbol{\theta}'|$. The mean number density of galaxies populating the new haloes is $N_\mathrm{h}N_\mathrm{g}/A$. If the new halo type is mixed with other haloes, such as ILM haloes, the *total* number density of galaxies, $\bar{n}_\mathrm{g}$, may be different. The one halo term is not affected by the presence of the other haloes apart from $\bar{n}_\mathrm{g}$.

The sum (B.2) vanishes for $\boldsymbol{\theta}_1\neq\boldsymbol{\theta}_2$ so that the only relevant contribution to the one-halo terms of $\mathcal{G}$ is, after exploiting the Dirac delta functions,

$$\begin{aligned}
\mathcal{G}^\mathrm{1h}(\vartheta_1,\vartheta_2,\phi_3) &= -\mathrm{e}^{-\mathrm{i}(\varphi_1+\varphi_2)}\bar{n}_\mathrm{g}^{-2}N_\mathrm{h}N_\mathrm{g}(N_\mathrm{g}-1)A^{-1}\int \mathrm{d}^2\theta\,P_\Delta(|\boldsymbol{\theta}+\boldsymbol{\theta}_{12}|,|\boldsymbol{\theta}|,|\boldsymbol{\theta}_{12}|)\,\overline{\gamma}_\mathrm{h}(\boldsymbol{\theta}_{32}+\boldsymbol{\theta}) \\
&= -\mathrm{e}^{-\mathrm{i}(\varphi_1+\varphi_2)}\bar{n}_\mathrm{g}^{-1}f_\mathrm{h}N_\mathrm{g}(N_\mathrm{g}-1)\int \mathrm{d}^2\theta\,P_\Delta(|\boldsymbol{\theta}+\boldsymbol{\theta}_{13}|,|\boldsymbol{\theta}+\boldsymbol{\theta}_{23}|,\vartheta_3)\,\overline{\gamma}_\mathrm{h}(\boldsymbol{\theta}) \\
&= \bar{n}_\mathrm{g}^{-1}f_\mathrm{h}N_\mathrm{g}(N_\mathrm{g}-1)\int \mathrm{d}\theta\,\theta\mathrm{d}\varphi\,P_\Delta(|\boldsymbol{\theta}+\boldsymbol{\theta}_{13}|,|\boldsymbol{\theta}+\boldsymbol{\theta}_{23}|,\vartheta_3)\mathrm{e}^{\mathrm{i}(2\varphi-\varphi_1-\varphi_2)}\,\overline{\gamma}_{\mathrm{t,h}}(\theta) \\
&= \bar{n}_\mathrm{g}^{-1}\,\mathrm{e}^{+2\mathrm{i}\phi_3}f_\mathrm{h}N_\mathrm{g}(N_\mathrm{g}-1)\int_0^\infty \mathrm{d}\theta\,\theta\overline{\gamma}_{\mathrm{t,h}}(\theta)\int_0^{2\pi}\mathrm{d}\varphi\,\cos(2\varphi)\,P_\Delta(\Upsilon(\vartheta_1,\theta,\varphi+\phi_3),\Upsilon(\vartheta_2,\theta,\varphi),\vartheta_3).
\end{aligned} \tag{B.6}$$

We used (24) for the definition of Υ. By $f_\mathrm{h} := N_\mathrm{h}/(A\bar{n}_\mathrm{g})$ we mean the ratio of new type haloes to the total number of galaxies; as usual, $\vartheta_3^2 = \vartheta_1^2+\vartheta_2^2-2\vartheta_1\vartheta_2\cos\phi_3$ is the separation of the lenses. If we add more haloes with, say, different shear profiles or numbers of galaxies N_g, we will obtain a sum of one-halo terms of the previous kind, all weighed with (i) their halo fractions f_h and (ii) number of galaxy pairs $N_\mathrm{g}(N_\mathrm{g}-1)$. ILM haloes have trivially $N_\mathrm{g}=1$, thus vanishing one-halo terms due to the absence of galaxy pairs. Moreover, if galaxies are unclustered inside their host haloes, $P_\Delta\sim$ const., one will also have a vanishing one-halo term. When the host haloes are not clustered as well, there will be no contribution to $\mathcal{G}$ at all.

Appendix C: General elliptical matter haloes and $G_\pm$

We consider a projected halo matter density profile with constant power law slope when averaged over annuli. The profiles have an elliptical shape with ellipticity $\epsilon_\mathrm{h} = (a^2 - b^2)/(a^2 + b^2)$; a, b are the sizes of the major and minor axis, respectively. Mandelbaum et al. (2006a) find for the shear profile corresponding to this matter density profile

$$\gamma_\mathrm{h}(\boldsymbol{\theta};\boldsymbol{\alpha}) = -\frac{A\delta\theta^{-\delta}}{2-\delta}\mathrm{e}^{2\mathrm{i}\varphi}(\gamma_\mathrm{t} + \mathrm{i}\gamma_\times); \gamma_\mathrm{t} := 1 + \frac{(\delta-2)(\delta^2-2\delta+4)}{\delta^2(\delta-4)}\frac{\epsilon_\mathrm{h}}{2}\cos(2\varphi); \gamma_\times := \frac{4(2-\delta)(1-\delta)}{\delta^2(\delta-4)}\frac{\epsilon_\mathrm{h}}{2}\sin(2\varphi), \tag{C.1}$$

where we denote by φ the polar angle of $\boldsymbol{\theta}$ and by A the amplitude of the shear. For simplicity, we work with the assumption that all haloes have the same ellipticity, power law index and amplitude. As the orientation of a halo is a-priori not known, we have to marginalise over the random orientation angle of the halo for correlator (41),

$$\overline{\gamma_\mathrm{t,h}}(\theta,\varphi) = \frac{A\delta\,\theta^{-\delta}}{\delta-2}, \tag{C.2}$$

$$\delta G_-^\mathrm{1h}(\vartheta_1,\vartheta_2,\phi_3) = \frac{\epsilon_\mathrm{h}^2}{8}f_-(\delta)\cos(2\phi_3), \tag{C.3}$$

$$\delta G_+^\mathrm{1h}(\vartheta_1,\vartheta_2,\phi_3) = \frac{\epsilon_\mathrm{h}^2}{8}f_+(\delta)\cos(2\phi_3) + \mathrm{i}\frac{\epsilon_\mathrm{h}^2}{8}g_+(\delta)\sin(2\phi_3), \tag{C.4}$$

with the auxiliary functions

$$f_-(x) := \frac{(x-2)^3(x+2)}{x^3(x-4)}; f_+(x) := \frac{(x^4-4x^3+28x^2-48x+32)(x-2)^2}{(x-4)^2x^4}; g_+(x) := \frac{(x-2)^2(x^3-3x^2+6x-4)}{(x-4)^2x^4}. \tag{C.5}$$

One has $f_+(\delta) = f_-(\delta) = 1$ and $g_+(\delta) = 0$ for a SIE ($\delta = 1$).

References

Bartelmann, M. 2010, Rev. Mod. Phys., 82, 331
Bartelmann, M., & Schneider, P. 2001, Phys. Rep., 340, 291
Bower, R. G., Benson, A. J., Malbon, R., et al. 2006, MNRAS, 370, 645
Brainerd, T. G., Blandford, R. D., & Smail, I. 1996, ApJ, 466, 623
Cooray, A., & Sheth, R. 2002, Phys. Rep., 372, 1
De Lucia, G., Poggianti, B. M., Aragón-Salamanca, A., et al. 2007, MNRAS, 374, 809
Dodelson, S. 2003, Modern cosmology (Academic Press) 2003, XIII + 440 p.
Fischer, P., McKay, T. A., Sheldon, E., et al. 2000, AJ, 120, 1198
Griffiths, R. E., Casertano, S., Im, M., & Ratnatunga, K. U. 1996, MNRAS, 282, 1159
Guzik, J., & Seljak, U. 2002, MNRAS, 335, 311
Hoekstra, H., Van Waerbeke, L., & Gladders, M. D. 2002, ApJ, 577, 604
Hoekstra, H., Yee, H. K. C., & Gladders, M. D. 2004, ApJ, 606, 67
Johnston, D. E. 2006, MNRAS, 367, 1222
Kaiser, N., & Squires, G. 1993, ApJ, 404, 441
Kleinheinrich, M., Rix, H.-W., Erben, T., et al. 2005, A&A, 439, 513
Laureijs, R., Amiaux, J., Arduini, S., et al. 2011 [arXiv:1110.3193]
Mandelbaum, R., Tasitsiomi, A., Seljak, U., Kravtsov, A. V., & Wechsler, R. H. 2005, MNRAS, 362, 1451
Mandelbaum, R., Hirata, C. M., Broderick, T., Seljak, U., & Brinkmann, J. 2006a, MNRAS, 370, 1008
Mandelbaum, R., Seljak, U., Kauffmann, G., Hirata, C. M., & Brinkmann, J. 2006b, MNRAS, 368, 715
McKay, T. A., Sheldon, E. S., Racusin, J., et al. 2001, unpublished [arXiv:0108013]
Parker, L. C., Hoekstra, H., Hudson, M. J., van Waerbeke, L., & Mellier, Y. 2007, ApJ, 669, 21
Peebles, P. J. E. 1980, The large-scale structure of the universe (USA: Princeton University Press)
Peebles, P. J. E. 1993, Principles of physical cosmology (Princeton University Press)
Pen, U.-L., Lu, T., van Waerbeke, L., & Mellier, Y. 2003, MNRAS, 346, 994
Scherrer, R. J., & Bertschinger, E. 1991, ApJ, 381, 349
Schneider, P. 2006, in Saas-Fee Advanced Course 33: Gravitational Lensing: Strong, Weak and Micro, eds. G. Meylan, P. Jetzer, P. North, P. Schneider, C. S. Kochanek, & J. Wambsganss, 269
Schneider, P., & Watts, P. 2005, A&A, 432, 783
Schrabback, T., Hartlap, J., & Joachimi, B. 2010, A&A, 516, A63
Seljak, U., & Warren, M. S. 2004, MNRAS, 355, 129
Sheldon, E. S., Johnston, D. E., Frieman, J. A., et al. 2004, AJ, 127, 2544
Simon, P., Hetterscheidt, M., Schirmer, M., et al. 2007, A&A, 461, 861
Simon, P., Watts, P., Schneider, P., et al. 2008, A&A, 479, 655
Tyson, J. A., Valdes, F., Jarvis, J. F., & Mills, Jr., A. P. 1984, ApJ, 281, L59
van Uitert, E., Hoekstra, H., Velander, M., et al. 2011, A&A, 534, A14
Weinberg, D. H., Davé, R., Katz, N., & Hernquist, L. 2004, ApJ, 601, 1